

RESEARCH ARTICLE

Changing freshwater contributions to the Arctic: A 90-year trend analysis (1981–2070)

Tricia A. Stadnyk^{1,2,*}, A. Tefs¹, M. Broesky², S. J. Déry³, P. G. Myers⁴, N. A. Ridenour⁴, K. Koenig⁵, L. Vonderbank⁶, and D. Gustafsson⁷

The pan-Arctic domain is undergoing some of Earth's most rapid and significant changes resulting from anthropogenic and climate-induced alteration of freshwater distribution. Changes in terrestrial freshwater discharge entering the Arctic Basin from pan-Arctic watersheds significantly impact oceanic circulation and sea ice dynamics. Historical streamflow records in high-latitude basins are often discontinuous (seasonal or with large temporal gaps) or sparse (poor spatial coverage), however, making trends from observed records difficult to quantify. Our objectives were to generate a more continuous 90-year record (1981–2070) of spatially distributed freshwater flux for the Arctic Basin (all Arctic draining rivers, including the Yukon), suitable for forcing ocean models, and to analyze the changing simulated trends in freshwater discharge across the domain. We established these data as valid during the historical period (1971–2015) and then used projected futures (preserving uncertainty by running a coupled climate-hydrologic ensemble) to analyze long-term (2021–2070) trends for major Arctic draining rivers. When compared to historic trends reported in the literature, we find that trends are projected to nearly double by 2070, with river discharge to the Arctic Basin increasing by 22% (on average) by 2070. We also find a significant trend toward earlier onset of spring freshet and a general flattening of the average annual hydrograph, with a trend toward decreasing seasonality of Arctic freshwater discharge with climate change and regulation combined. The coupled climate-hydrologic ensemble was then used to force an ocean circulation model to simulate freshwater content and thermohaline circulation. This research provides the marine research community with a daily time series of historic and projected freshwater discharge suitable for forcing sea ice and ocean models. Although important, this work is only a first step in mapping the impacts of climate change on the pan-Arctic region.

Keywords: Arctic, Freshwater discharge, Climate change, Trend analysis, Ocean modeling, BaySys

1. Introduction

The Arctic is currently in a period of rapid transition owing to amplified climate change. Although average global warming has reached slightly above 1 °C, the Arctic region is already experiencing up to 2 °C warming and is highly sensitive to climate change. Warming in polar regions is projected to increase at rates of 1.5–4.5 times greater than the remainder of the Northern Hemisphere (Holland and Bitz, 2003). Climate simulations over Hudson Bay show the northern Foxe Basin to be 0.64 °C–1.65 °C warmer than lower-latitude subregions (i.e., Nelson River), and up to 40%–136% wetter, on average, by the 2050s and

2070s, respectively (Braun et al., n.d.). Approximately 40 million people would be affected by hydrological changes in Arctic rivers, particularly in regions like Canada where more than 60% of the landmass drains northward (Déry et al., 2011).

Freshwater discharge to the Arctic Basin impacts ocean salinity as well as marine processes including sea ice formation and thermohaline circulation. Oceanographers typically define freshwater as the amount of zero salinity water contained in a volume compared to a reference salinity; Arctic Ocean freshwater budgets have been computed and updated since Aagaard and Carmack (1989).

¹ Department of Geography, University of Calgary, Calgary, Alberta, Canada

² Department of Civil Engineering, University of Manitoba, Winnipeg, Manitoba, Canada

³ Environmental Science and Engineering Program, University of Northern British Columbia, Prince George, British Columbia, Canada

⁴ Department of Earth and Atmospheric Sciences, University of Alberta, Edmonton, Alberta, Canada

⁵ Manitoba Hydro, Hydrologic and Hydroclimatic Studies Section, Winnipeg, Manitoba, Canada

⁶ Department of Civil Engineering, University of Calgary, Calgary, Alberta, Canada

⁷ Hydrology Research Unit, Swedish Meteorological and Hydrological Institute, Norrköping, Folkborgsvägen, Sweden

* Corresponding author:
Email: tricia.stadnyk@ucalgary.ca

Recent work (e.g., Haine et al., 2015) suggests that during the period 1980–2000, the Arctic Ocean had a freshwater storage of around 93,000 km³ relative to the Basin's average salinity of 34.8, with input from Bering Strait, precipitation minus evaporation, and runoff being balanced by exchange with the Atlantic Ocean. Haine et al. (2015) suggest that river runoff is the largest of the freshwater sources. The end result is a highly stratified basin, with a coastal riverine domain (Carmack et al., 2015), significant freshwater storage in the Beaufort Gyre (e.g., Proshutinsky et al., 2019), and transport across the Basin in the Transpolar Drift.

Arctic freshwater content has been increasing significantly over recent years (e.g., Haine et al., 2015), which is consistent with observations of enhanced river discharge (e.g., Morison et al., 2012), as well as with increased exchange at Bering Strait (Woodgate et al., 2006). Export of low salinity Arctic water has been shown to have significant impacts on the Atlantic Ocean in the past (e.g., Dickson et al., 1988; Curry and Mauritzen, 2005). Thus, some authors have speculated that future increases in Arctic freshening and export might potentially impact deep water formation in the Labrador Sea (e.g., Yang et al., 2016) and the Atlantic meridional overturning circulation (AMOC; e.g., Wang et al., 2018), both of which regulate global climate patterns.

Across Arctic-draining continental landmasses, changes in air temperature and precipitation affect both the amount and timing of streamflow and runoff production. Climate models anticipate the pan-Arctic domain becoming wetter in a warmer world (MacDonald et al., 2018). Studies of Arctic streamflow are now more frequent, with observations ubiquitously indicating increasing river discharge in recent years (Peterson et al., 2002; Arnell, 2005; Bring et al., 2017). Several studies have examined the largest Arctic rivers, with some focusing on differences between North American and Eurasian flows (Gelfan et al., 2017), reporting the largest increases occurring around Alaska (Arnell, 2005). Increased moisture transport and convergence over large terrestrial basins may explain, in part, the sharp increases observed in Eurasian discharge (Zhang et al., 2013). Discharge from rivers in northern Canada declined significantly until 1990 and subsequently began to increase, following Eurasian trends (Déry et al., 2009). What led to this reversal in trend and its persistence, or whether it is part of (inter)decadal variability within the climate system, is not known.

Changes in continental flow regimes have also been imposed by increasing anthropogenic development and river control due to regulation (Dynesius and Nilsson, 1994), defined here as the control of river stage or discharge for human consumptive or energy production needs. In some cases, regulation at continental scales has been identified as a more significant influence than climate change (Arheimer et al., 2017). Both climate change and regulation are likely to increase winter low flows, contributing to decreased freshwater seasonality. Global climate models (GCMs) project atmospheric warming which can increase precipitation and evapotranspiration across the Northern Hemisphere and may also contribute

to earlier and more frequent melt events, resulting in a lower spring freshet. Large water infrastructure involved in regulation, such as large dams and reservoirs, is known to alter the seasonality of flow (Déry et al., 2018).

Permafrost thaw and forest fires under climate change are also anticipated to have a significant impact on pan-Arctic discharge (McClelland et al., 2004). Processes like evapotranspiration and precipitation that are closely interconnected determine the amount of runoff produced from a region. Generally, evapotranspiration returns less water into the air than what is precipitated, particularly in the cool, vegetation-sparse Arctic. As the atmosphere warms, its water-holding capacity increases, which potentially results in increased precipitation and enhanced vegetation growth. Transpiration amounts are highly dependent on vegetation cover and soil type, adding increased uncertainty under future projections. Observed increases in winter flow have been attributed to increasing late autumn rain, permafrost thaw, and increasing groundwater contributions to runoff (Bring and Destouni, 2011). These “alternative mechanisms” affect the seasonality of flow but are typically considered as not significant enough to account for increasing freshwater volumes (Durocher et al., 2019). McClelland et al. (2004) concluded the positive trends in 20th-century Eurasian discharge could not be solely explained by permafrost degradation, forest fire activity, or dams.

Owing to the large contributing area, remoteness of the pan-Arctic domain, and significant gaps in observational records, the reasons for, and impacts of, changing freshwater discharge on the Arctic marine system are largely unknown. Although some work on this topic has occurred within the oceanographic community, simulations have relied largely on simplified runoff fields. Nummelin et al. (2015) used a simple one-dimensional column model to show that future increases in Arctic runoff will likely lead to enhanced stratification, with enhanced warming below the stratified layer. With idealized runoff perturbations (increases) ranging from 10% to 150%, Nummelin et al. (2016) showed that their idealized results were robust with a coarse resolution climate model. Pemberton and Nilsson (2016) performed runoff sensitivity experiments in an ocean/sea-ice model that enhanced runoff and shallowed the halocline, while also modifying the Atlantic water inflow. Lambert et al. (2019) used a climate response function approach to show the diffusion of heat and salt in the Arctic increased under enhanced runoff, eventually leading to enhanced advective imports of salt and heat into the Arctic.

The objective of this study was to generate a more temporally and spatially continuous 90-year record of Arctic freshwater discharge to (1) identify significant spatial and temporal trends in pan-Arctic freshwater discharge, (2) identify the influence of river regulation on identified trends, and (3) assess the impact of dynamic freshwater forcing on long-term simulation of ocean freshwater content. We derived a 90-year record of freshwater discharge to the pan-Arctic domain using the Arctic-Hydrological Predictions for the Environment (A-HYPE) hydrological model across both historic and future periods

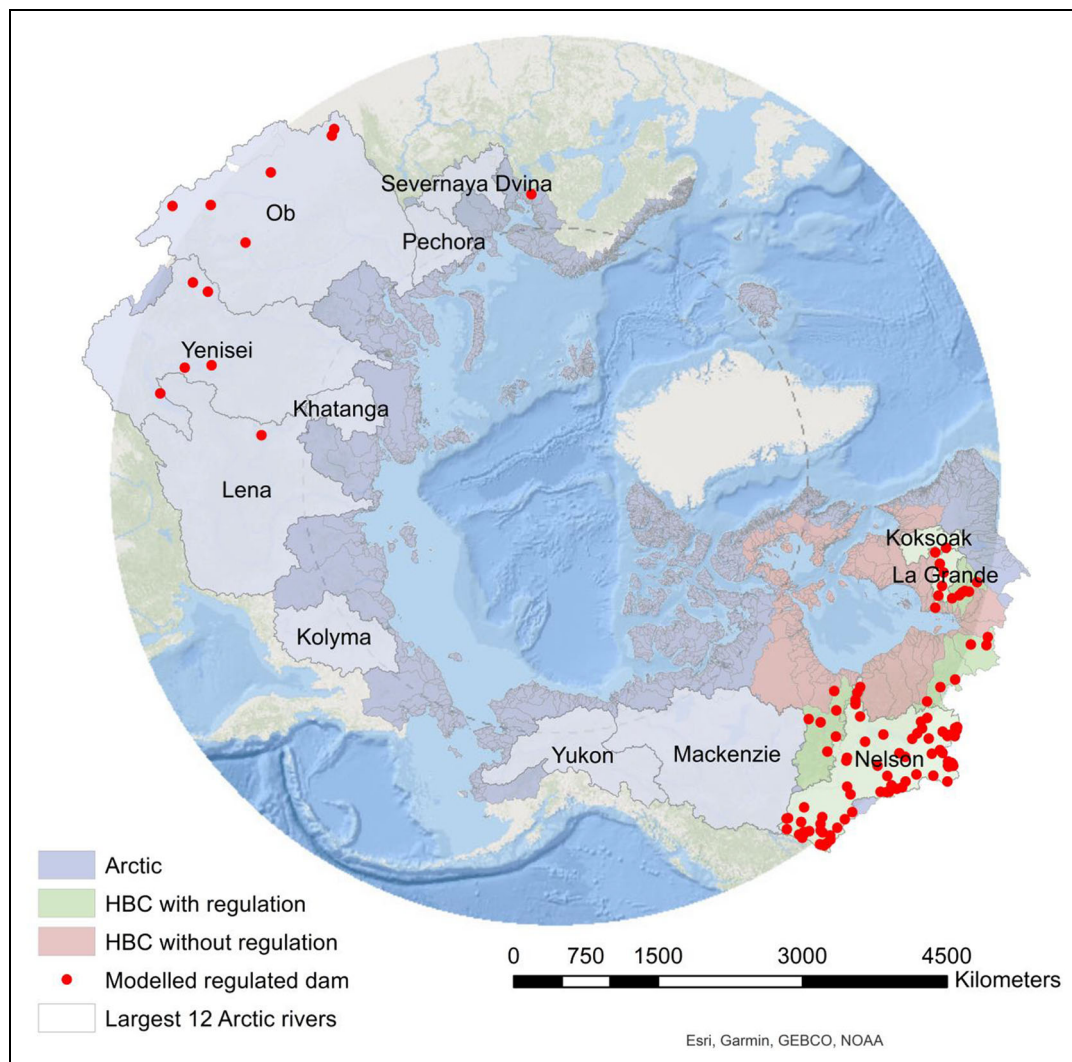


Figure 1. Pan-Arctic domain indicating 12 largest river basins (by average annual volume) simulated by Arctic-Hydrological Predictions for the Environment. Basins in red contain no explicit regulation modeling and drain into the Hudson Bay Complex (HBC), basins in green contain regulation modeling and drain into the HBC, and basins in blue contain limited explicit regulation modeling and drain directly to the Arctic Ocean. Dam locations (red dots) are those modeled with some degree of regulation. DOI: <https://doi.org/10.1525/elementa.2020.00098.f1>

(1981–2070). We applied five GCM simulations to drive the pan-Arctic hydrologic model and generate a continuous 90-year sequence of freshwater discharge. Focusing on the 12 largest Arctic rivers (by volume), we assessed overall and moving-window 30-year period trends in freshwater inflow, quantiles of river discharge, and the net impact on ocean salinity in the Arctic Ocean. This work was undertaken as part of the BaySys project and was the first step in providing a more continuous and spatially congruent freshwater discharge product for long-term simulations within the Nucleus for European Modelling of the Ocean (NEMO) Ocean model, although this forcing data set would work for any ocean general circulation model.

2. Pan-Arctic drainage basin

The total land area contributing water to the Arctic Ocean and its adjacent seas is estimated to be 23.1 million km² spanning three continents and seven countries (**Figure 1**). Relative to other continental drainage basins, the pan-

Arctic domain generates a high amount of runoff (and therefore river discharge) relative to its land area. The bulk of the pan-Arctic discharge originates from the Eurasian and North American landmasses, contributing directly to the Arctic Ocean, with some exceptions. For example, the Yukon River is considered one of the 12 largest (by volume) pan-Arctic rivers but does not contribute directly to the Arctic Ocean, instead entering the Pacific Ocean south of Bering Strait; we include the Yukon River in our analyses, however, because it is part of the terrestrial pan-Arctic basin. The 12 largest pan-Arctic rivers (by volume) are listed in **Table 1**, along with their observed mean annual discharge (outlet contributions, without upstream diversion), percentage of total pan-Arctic discharge, and contributing area. The Koksoak is the 12th ranked river because its estimated “virgin mean annual discharge” is 2,420 m³ s⁻¹ (Dynesius and Nilsson, 1994), which is what A-HYPE approximates but is considerably less than what is observed. Together, these 12 rivers represent 57% of total

Table 1. Twelve largest pan-Arctic rivers (by volume) simulated in A-HYPE. DOI: <https://doi.org/10.1525/elementa.2020.00098.t1>

River Basin	Observed ^a Mean Daily Discharge (m ³ s ⁻¹)	Estimated Drainage Area ^b (km ²)	Continent	Contribution to Total Pan-Arctic Discharge (%)
Yenisey	19,499	2,442,735	Eurasia	10.4
Lena	17,773	2,418,974	Eurasia	9.5
Ob	12,889	2,917,508	Eurasia	11.0
Mackenzie	9,211	1,717,754	North America	5.7
Khatanga	6,757	264,999	Eurasia	0.8
Yukon	6,576	820,856	North America	3.4
Pechora	4,823	312,041	Eurasia	2.3
Severnaya Dvina	3,416	350,496	Eurasia	2.6
Nelson	3,343	1,111,890	North America	1.6
Kolyma	3,234	533,013	Eurasia	1.7
La Grande Rivière	3,039	100,729	North America	1.2
Koksoak	1,458 ^b	136,262	North America	0.6

A-HYPE = Arctic-Hydrological Predictions for the Environment.

^aObserved discharge represents what is actually recorded at a gauge location and includes upstream diversion, which in this case is not included in A-HYPE.

^bBased on outlet discharge, which includes (for some rivers) extrapolating observed gauge volumes and areas to downstream outlet using a blend of Hydrological Cycle Observing System and Global Runoff Data Centre data. Drainage areas are therefore reported as those estimated by the A-HYPE model and do not include upstream diversions.

pan-Arctic discharge from 17.5 million km² of the terrestrial drainage area (or 81% of total Arctic basin discharge from 82% of the pan-Arctic domain).

Greenland was excluded from our definition of the pan-Arctic drainage basin because it is an ice sheet-dominated landscape with little ice-free area (i.e., approximately 20%). Tundra-derived runoff was estimated by Bamber et al. (2012) to be only approximately 10% of the total freshwater flux from Greenland. In recent decades, however, glacier melt has been thought to contribute substantial freshwater runoff from the Greenland coast (Dukhovskoy et al., 2016; Bamber et al., 2018). Studies validating the role of Greenland-derived freshwater in Arctic Ocean thermohaline circulation are few (Bamber et al., 2012; Straneo and Heimbach, 2013; Yang et al., 2016). Greenland was omitted from our domain of analysis, similarly to other freshwater studies in the Arctic (Bring et al., 2017).

The majority of pan-Arctic river basins exhibit typical polar climates with low average annual and mean variability in temperature and significant cloud cover (60%–80%; Serreze and Barry, 2014). At these high latitudes, polar night exists during winter, along with cold temperatures and relatively stable weather systems. Summers bring more frequent cyclones and instability, with possible rain or snow, and are characterized by midnight sun. Parts of these river basins, however, have their headwaters at much lower latitudes, which are characterized by boreal and prairie ecoregions with typical continental climates. The majority of the pan-Arctic basin reside within the polar and cold Köppen Geiger (KPN) classifications (Kottek et al., 2006)

as defined from the historic period (1981–2015), though recent studies suggest that these classifications may change in future periods (Rubel and Kottek, 2010). KPN classifications are used to define and parameterize processes within the HYPE model (Arheimer et al., 2020).

Several of the largest pan-Arctic rivers, both Eurasian and North American, are affected significantly by river regulation, complicating freshwater discharge modeling and trend analyses (Vörösmarty et al., 2003; Shiklomanov and Lammers, 2009; Grill et al., 2015, 2019). Within the pan-Arctic domain lies the Hudson Bay Drainage Basin (HBDB), a terrestrial basin encompassing 3.98 million km² or roughly 15% of the total pan-Arctic domain. This subregion drains nearly one-third of the Canadian continental landmass and represents the study area for the BaySys group of projects. An extensive study of the relative impacts of climate change and human regulation was conducted within this subregion, including for freshwater discharge, as part of the BaySys project (Tefs, 2018; Tefs et al., 2021). To better understand the impacts of pan-Arctic domain river regulation on trend detection and analysis, we undertook a comparison of trends from regulated and nonregulated rivers within the HBDB subregion (see **Figure 1**).

3. Methods

To generate a 90-year record of freshwater discharge across the entire pan-Arctic domain (1981–2070), we combined over 20 years of observed hydrometric records obtained from the Arctic-Hydrological Cycle Observing

Table 2. GCM-RCP combinations from CMIP5 used in the pan-Arctic analysis. DOI: <https://doi.org/10.1525/elementa.2020.00098.t2>

GCM Run	Description	RCP	Resolution	Organization
Geophysical Fluid Dynamics Laboratory (GFDL)-CM3	GFDL coupled physical model, version 3	4.5	2° × 2°	National Oceanic and Atmospheric Administration/GFDL
MIROC5	Model for the interdisciplinary research on climate, version 5	4.5 8.5	1.4° × 1.4° 1.4° × 1.4°	Atmosphere and Ocean Research Institute, National Institute for Environmental Studies, and Japan Agency for Marine-Earth Science and Technology
Meteorological Research Institute (MRI)-Canadian Global Climate Model (CGCM3)	MRI model coupled with the CGCM, version 3	4.5 8.5	1° × 1° 1° × 1°	MRI, Japan Meteorological Agency, Japan

CMIP5 = Coupled Model Intercomparison Project Phase 5; GCM = global climate model; RCP = representative concentration pathway.

System (HYCOS) network coinciding with our model historical evaluation period (1971–2016; <https://hydrohub.wmo.int/en/projects/Arctic-HYCOS>), with modeled discharge produced using the Swedish Meteorological and Hydrologic Institute (SMHI) A-HYPE model adapted from Andersson et al. (2015). A-HYPE was forced by the HydroGFDv2 climate reanalysis (Berg et al., 2018) and an ensemble of 14 GCM simulations corresponding to the historic period (1981–2010). Future time series of freshwater discharge was generated by forcing A-HYPE with an ensemble of future climate scenarios (2011–2070). A-HYPE was then used to drive an ocean model to examine the impact of dynamic freshwater forcing on long-term simulation of marine freshwater content.

3.1. Climate data forcing

The ensemble of five GCMs and representative concentration pathway (RCP) combinations selected to represent future climatic variability were derived from the Coupled Model Intercomparison Project Phase 5 suite of experiments and designed to maximize climatic variability across the Hudson Bay domain for the BaySys project (Braun et al., n.d.). Three GCMs and two RCPs (RCP 4.5 and 8.5) were used (Table 2). A smaller selection of climate models was adopted for this research due to the requirement for additional meteorological variables needed to drive the ocean model, the large size of the domain required for ocean modeling (North Atlantic), and the feasibility in computational demand owing to the large and relatively high-resolution spatial domain being modeled.

Climate data were downscaled and bias-corrected by Uranos using the methodology recommended by Chen et al. (2013; Braun et al., n.d.). For the A-HYPE domain, temperature (minimum, maximum, and mean) and precipitation variables were bias-corrected to HydroGFDv2 (Section 3.2) using quantile mapping. Ocean modeling required temperature, precipitation (rain and snow), wind component velocities (u , v at 10 m), and incoming (short- and long-wave) radiation. Only temperature, precipitation, and wind were bias-corrected over the ocean domain. Historical analyses in this study were forced by European

Centre for Medium-Range Weather Forecasts Re-Analysis (ERA) interim reanalysis across a ¼ degree regional configuration of the Arctic and North Hemisphere Atlantic domain over the ocean, which is consistent with the HydroGFDv2 background product used for terrestrial modeling. A summary of the climate simulation selection criteria and bias-correction methodology are provided in Stadnyk et al. (2019).

3.2. Observational data sets

Observation data sets form an important component of our analyses and were obtained from a variety of data repositories to provide a continuous and contiguous record over the domain of analysis. Hydrometric data were obtained from various agencies through the World Meteorological Organization's Arctic hydrometric station network. These data are supplemented by a Canadian gap-filled hydrometric data set derived from 1964 to 2013 that used the observed Canadian daily river discharge from the Water Survey of Canada's Hydrometric Database (<http://www.ec.gc.ca/rhc-wsc/>) and the Centre d'Expertise Hydrique for northern Québec and Nunavik (<http://www.cehq.gouv.qc.ca/suivihydro/default.asp>). Additional discharge data for the Canadian network were provided by Hydro-Québec, Manitoba Hydro, and Ontario Power Generation for our regulated river analysis.

Daily air temperature and precipitation from HydroGFDv2, or version 2.0 (Berg et al., 2018), were used to force the hydrological model at a spatial resolution of 0.5°. Global forcing data are climate reanalyses combining observations and the ERA40 (1957–2002) and ERA-Interim (1979–2019) data to derive a continuous record of global temperature and precipitation data (1960–2018). These data were selected because they provide global coverage in near real-time and are designed for hydrologic modeling.

The “Dai and Trenberth” (Dai, 2017) global river flow and continental discharge data provide observed continental discharge for 925 of the world's largest rivers. These data contain time series of monthly river discharge observed at the farthest downstream (outlet) stations and include long-term mean discharge beginning in 1948 and

Table 3. A-HYPE process-based calibration data summary. DOI: <https://doi.org/10.1525/elementa.2020.00098.t3>

Process	Source	Source	Selected Variable (Unit)
Snowmelt	Former Soviet Union Snow Courses	www.nsidc.org	Snow water equivalent (mm)
Glaciers	RGI v4; World Glacier Monitoring Service	(Huss and Farinotti, 2012); www.wgms.ch	Glacial area (km ²); Ice cap volume (m ³)
Evapotranspiration	FluxNet	Fluxnet.ornl.gov	Evapotranspiration (mm)

A-HYPE = Arctic-Hydrological Predictions for the Environment.

up to 2016, at the time of this study. Many gauges contain significant temporal gaps; therefore, these data are available “as is” (noninfilled) or as a gap-filled monthly record (Dai et al., 2009). Infilled records used the Community Land Model (version 3) and linear regression to address significant observational gaps. For this study, we used the infilled Dai and Trenberth data to drive the regional configuration of the NEMO model.

For calibration of A-HYPE, SMHI used 79 of the HYCOS Arctic-draining (outlet) hydrometric gauges and 540 of the Arctic-HYCOS upstream stations over the original simulation period (1971–2013). In this study, we extend the modeling period to the end of 2015 and add data from Déry et al. (2016) and the Global Runoff Data Centre (GRDC; https://www.bafg.de/GRDC/EN/01_GRDC/grdc_node.html) rivers database for additional validation.

3.3. A-HYPE modeling

3.3.1. Arctic HYPE

The A-HYPE implementation of the HYPE (Lindström et al., 2010) model was initially developed by SMHI. The A-HYPE implementation covers 23 million km² of the global continental landmass draining poleward, toward the Arctic Ocean, divided into 32,599 subbasins with approximately 700 km² horizontal resolution. For this research, a modified version of the model was generated by the University of Calgary Hydrologic Analysis Laboratory that included improved lake calibration, a frozen soil routine, and a regulation (reservoir) model for the HBDB (Stadnyk et al., 2020). This revised implementation of A-HYPE was used to generate daily streamflow for the pan-Arctic domain (Figure 1), driven by the HydroGFDv2 reanalysis. A-HYPE model output is characterized by continuous-in-time spectra (over a long period of time) and contiguous spatial extent (as opposed to flow outlets only) across the pan-Arctic domain. Model output was analyzed across three 30-year time periods: historic baseline (1981–2010), near future (2021–2050), and far future (2041–2070), though results were produced by continuous simulation over the period 1971–2070. The historic period 1971–2015 was used for model calibration and validation, as described in the following section.

3.3.2. Model calibration and validation

The A-HYPE model was calibrated by SMHI (2020) using hydrometric data obtained (in order of preferred source)

from R-ArcticNet (<http://www.r-arcticnet.sr.unh.edu/v4.0/>), the GRDC, and data from national hydrometric agencies (Canada, United States, Finland, Norway, and Iceland). Within the pan-Arctic region, there were a total of 1,349 gauging stations, with approximately 30% (or more in recent years) of the pan-Arctic being ungauged. Details on A-HYPE model calibration, spatially dependent summaries of model performance, and the calibration methodology are available from the HypeWeb (<https://hypeweb.smhi.se/explore-water/model-performances/>). Additional calibration was performed for specific hydrologic processes using open-source global data sets (Table 3).

Owing to the size and interjurisdictional nature of the pan-Arctic domain, utilizing one source of data for either calibration or validation was not possible, and data coverage and quality were highly variable. We utilized a regional approach to model validation that leveraged specific data (not used for calibration) representing distinct regions of the pan-Arctic domain. We conducted model validation for this study using 10 Arctic-HYCOS Arctic-draining (outlet) hydrometric gauges, an additional 31 GRDC stations, and a regional subset of 34 Arctic-draining outlet stations derived by Déry et al. (2016), totaling 75 stations across the pan-Arctic domain. Our validation covered approximately two-thirds (67%) of the total discharge to the Arctic Ocean. This pseudo-observational data set (hereafter referred to as “discharge observations”) formed the hydrometric network used for model validation in our study; we specify the data source used for validation at each gauge location (e.g., Figure 2).

As part of the BaySys project, a new configuration and recalibration of the A-HYPE model was conducted for the HBDB and is summarized in Stadnyk et al. (2020). River regulation, frozen soil processes, and lake routing were revised within the Canadian domain (Stadnyk et al., 2020), which is utilized in this study as well. Here, we evaluated model performance across the pan-Arctic domain using daily discharge aggregated to a monthly timescale where we computed statistics for our 75 validation gauges. We computed the Nash–Sutcliffe efficiency (NSE; Nash and Sutcliffe, 1970: Equation 1), Kling–Gupta efficiency (KGE; Gupta et al., 2009), and individual KGE components (Equations 3–5) over the historic period T (1971–2015), with entries x at time t , for both observed time series o and simulated time series

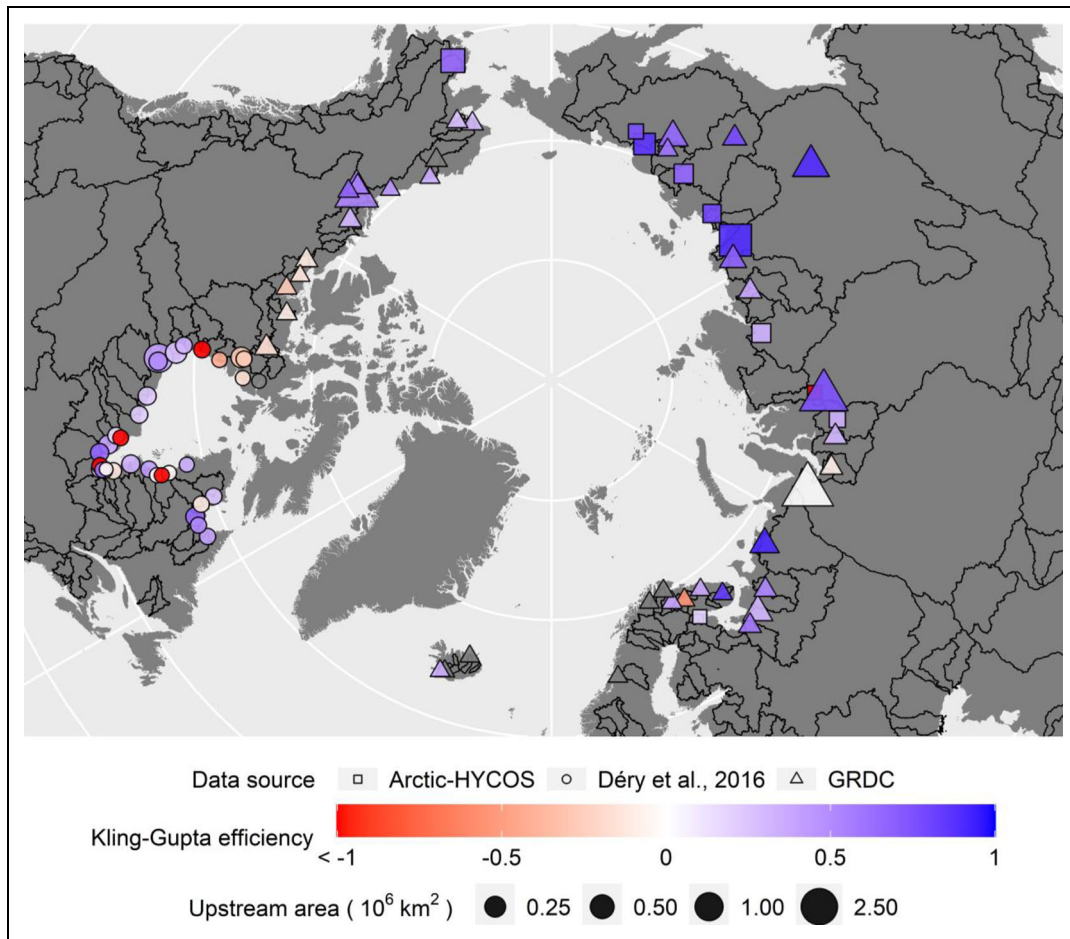


Figure 2. Modeled Kling–Gupta efficiency (KGE) of monthly discharge for 74 pan-Arctic gauges. Modeled KGE by major Arctic drainage basin outlet ($n = 74$, mean monthly discharge computed from daily simulation, 1971–2015; gauged station details listed in Table S1) for error components of KGE provided in Equations 2–4 and Figure S1. Scale is by upstream area (in million km^2); shape indicates observed data source, DERY = Déry et al., (2016); GRDC = Global Runoff Data Centre; HYCOS = Arctic- Hydrological Cycle Observing System. DOI: <https://doi.org/10.1525/elementa.2020.00098.f2>

s, each with their own mean μ , standard deviation σ , and coefficient of variation cov.

$$\text{NSE} = 1 - \frac{\sum_{t=1}^T (x_{s,t} - x_{o,t})^2}{\sum_{t=1}^T (x_{o,t} - \mu_o)^2}, \quad (1)$$

$$\beta = \frac{\mu_s}{\mu_o} - 1; \text{PBias}_\mu = \beta \times 100\%, \quad (2)$$

$$\alpha = \frac{\sigma_s}{\sigma_o} - 1; \text{PBias}_\sigma = \alpha \times 100\%, \quad (3)$$

$$\text{CC} = \frac{\text{cov}(X_o, X_s)}{\sigma_s \sigma_o}, \quad (4)$$

$$\text{KGE} = 1 - \sqrt{(\text{CC} - 1)^2 + \beta^2 + \alpha^2}. \quad (5)$$

Figure 2 summarizes model performance (KGE) at the Arctic-draining outlets of major rivers within the pan-Arctic domain, classified by mean annual flow (KGE component errors provided in Figure S1; validation scores for all gauges, in Table S1). The model performs “satisfactorily” or better at 30% of the gauges at the monthly timescale according to model performance criteria from Moriasi et al. (2016; i.e., $\text{NSE} > 0.50$ and BIAS, or

relative error of the mean ($\leq 15\%$). Average KGE for the Arctic-draining stations (HYCOS and GRDC; 61% of total pan-Arctic discharge) on a monthly timescale was 0.30, with a correlation of .73 between simulated and observed records (**Figure 2**). The worst performing stations ($\text{KGE} < 0.3$) contribute 16.5% of the total freshwater discharge from the pan-Arctic domain. Performance within the regional subset stations (Déry et al., 2016; approximately 9% of total pan-Arctic discharge) was lower, likely impacted by river regulation comprising $> 50\%$ of the discharge into the HBDB (Déry et al., 2018). Strong correlation between the simulated and observed data was seen across the domain, with more than 75% of the gauges having correlations greater than .5 (Figure S1d) and an average correlation of .73 overall (Figure S1a). Much of the simulation error was derived from variance and timing (Figure S1b and c), which is not surprising considering many of the large rivers are regulated regimes that are affecting seasonal (and monthly) freshwater discharge.

On an annual basis, gauges with lowest performance cumulatively contain $< 2\%$ of the total mean monthly discharge to the Arctic system, with 0.5% from Arctic subbasins contributing directly to the Arctic Ocean, and

Table 4. Worst performing rivers, as simulated by revised A-HYPE using mean monthly observed flow statistics, and their percentage of total discharge to the Arctic Ocean (1971–2015). DOI: <https://doi.org/10.1525/elementa.2020.00098.t4>

River ^a	Drainage Area (km ²)	KEG ^b	NSE ^b	Relative Error of the Mean (%)	Correlation Coefficient	Percentage of Total Drainage Area (%)	Percentage of Total Mean Observed ^c Flow (%)
Rivière Harricana	33,873	-8.91	-192.47	887.6	0.61	0.19	0.28
Thlewiaza and Tha-anne Rivers	49,599	-1.88	-12.92	-22.8	0.21	0.27	0.09
Rivière a l'Eau Claire	12,388	-1.49	-11.12	29.4	0.17	0.07	0.05
Ekwan River	21,546	-1.46	-6.66	192.5	0.41	0.12	0.12
Fergusson River	15,556	-0.42	-0.34	-73.8	0.17	0.09	0.01
Thelon and Kazan Rivers	246,371	-0.29	-0.86	-64.6	0.01	1.36	0.24
Quoich River	29,883	-0.27	-0.13	-80.7	0.55	0.16	0.02
Lorillard River	11,432	-0.17	0.03	-75.3	0.64	0.06	0.01
Rivière aux Feuilles	38,684	-0.11	-0.27	-61.1	0.37	0.21	0.11
Rivière Nastapoka	12,417	-0.06	-1.80	-62.1	0.26	0.07	0.05
Rivière Pontax	3,020	-0.04	-0.16	-46.5	0.68	0.02	0.03
Subtotal HBC	474,769	-0.66	-1.98	12.4	0.40	2.6	1.01
Khantaika at Shnezhnogorsk	29,814	-3.24	-9.30	405.8	0.34	0.16	0.18
Tuloma At Verkhne-Tulomskaya	17,458	-0.39	-3.77	-6.4	0.16	0.10	0.10
Burnside River near the mouth	17,210	-0.32	-0.17	-70.5	0.30	0.09	0.03
Ellice River near the mouth	16,739	-0.21	-0.02	-65.0	0.36	0.09	0.02
Tree River near the mouth	6,067	-0.21	-0.20	-56.4	0.36	0.03	0.01
Back River above Hermann River	88,092	-0.16	-0.07	-57.0	0.60	0.48	0.14
Coppermine River above Copper Creek	45,600	-0.10	-0.34	-63.6	0.71	0.25	0.07
Subtotal Arctic	220,980	-1.37	-20.6	56.6	0.37	1.2	0.54
Total	695,749	-1.10	-13.4	39.4	0.38	3.8	1.55

A-HYPE = Arctic-Hydrological Predictions for the Environment; KGE = Kling–Gupta efficiency; NSE = Nash–Sutcliffe efficiency.

^aWorst defined by any gauges reporting KGE < 0; KGE was used for model calibration.

^bStatistics computed on daily time series averaged monthly using Equations 1 through 5.

^cObserved data from Déry et al. (2016) and outlet-adjusted GRDC and Arctic-HYCOS data.

1% from Hudson Bay Complex (HBC) basins, primarily the northern and eastern HBC regions (**Table 4**). Several of the worst-performing rivers likely freeze to the bed in winter and therefore may have zero flow for up to 6 months or longer each year. The majority of the worst performing rivers have smaller drainage areas (average area of 38,653 km² relative to the average pan-Arctic subbasin area of >309,000 km²) and are likely subject to aufeis (overflow ice) that contributes to late summer flow (Markarieva et al., 2019).

3.4. Regulated and nonregulated systems

Anthropogenic water management plays an important role in many of the rivers terminating at the Arctic Basin. Impacts include flattened average annual hydrographs,

altering interannual variability and increasing weekly periodicity (Déry et al., 2018). Regulation in the original version of A-HYPE simulated discharge optimally at the seasonal timescale (Arheimer et al., 2017). In the revised A-HYPE model, regulation is incorporated at 155 points, simulating irrigation, water supply, flood control, or hydroelectric production. For the BaySys group of projects, two regulated complexes (Nelson–Churchill River Basin [NCRB] and the La Grande Rivière Complex [LGRC]) use more explicit regulation modeling, in cooperation with industrial partners (Manitoba Hydro and Hydro-Québec). Although these two regulated basins make up only 7.5% (1.8 million km²) of the total pan-Arctic Basin drainage region, they contribute 4.8% of the discharge (by volume) and contain 55% (85 of 155) of A-HYPE regulation points.

Additional regulation was added by Tefs (2018) for the HBDB in the NCRB and LGRC to address known weaknesses in simulating weekly or subweekly regulated discharge, or hydropeaking effects (Arheimer and Lindström, 2014; Donnelly et al., 2016). Storage and safety-driven simulated regulation is embedded at 10 points in the NCRB and was provided by Hydro-Québec collaborators at 12 points within the LGRC, driven by upstream net basin supply from HYPE (described in Tefs et al., 2021). For this study, we compared regulated and nonregulated systems for three cluster regions: regulated HBC (Nelson, Churchill, La Grande Rivière, Rupert, Eastmain, Koksoak, Grande Rivière de la Baleine, Moose, and Albany: HBC_{REG}), primarily nonregulated HBC (remaining rivers draining into the HBC: HBC_{NOREG}), and the entire Arctic Ocean domain simulated by A-HYPE with the revised HBDB domain.

A renaturalized model for the HBC was also developed as part of the BaySys project (Tefs et al., 2018), allowing comparison between regulated regimes and their “renaturalized” counterparts (under the same climate conditions) with the assumption that regulation had never been imposed on the river. A second version of the HBC HYPE model computed outflow for 86 regulated reservoirs (Figure 1) which were reverted to lakes in natural states (Tefs, 2018). For all regulation points, this computation included removing time-dependent, regulated storage-outflow relationships and replacing these with a power relationship of stage-to-discharge: $outflow = a (stage - outlet\ height)^b$. Parameters for the natural stage-discharge relationship (a and b) were fit from predevelopment water level and streamflow records from Water Survey of Canada. At 16 locations, the renaturalization further included editing landcover classes to reverse flooding caused by hydroelectric reservoirs. Pre- and postdevelopment reservoir flooded extents were computed from surveyed data provided by Hydro-Québec. Further details about the renaturalized model are provided in Tefs (2018).

3.5. Statistical analyses

A-HYPE was used to generate runoff and discharge across the entire pan-Arctic domain, for all Arctic-draining basins. To analyze and assess regional changes in time and space, we selected 12 of the largest (by volume) Arctic-draining rivers (having observed discharge) and performed more detailed spatial and temporal statistical change analyses.

3.5.1. Trend analysis

The Mann–Kendall test (Mann, 1945; Kendall, 1975) was employed with prewhitening (Yue et al., 2002) when lag 1 autocorrelation in daily, monthly, or annual time series ($P < 0.05$) was detected; this nonparametric, robust approach was used to detect monotonic trends in hydroclimatic variables. Both the magnitude and statistical significance of the trends were inferred from the Mann–Kendall test, and their field significance established using a Monte Carlo approach (Burn and Hag Elnur, 2002). Trend analyses were performed on daily discharge data across water years to reveal potential changes in spring freshet timing, late

summer recession, and winter low flow events for the 12 largest Arctic rivers (Figure 1) and each climate scenario. Trends were normalized by mean flow to facilitate inter-comparison. Interdecadal periodicity was analyzed using a moving window approach, beginning at the start of each decade, to capture changes in trends through time. Trends were averaged daily for each period of analysis for a given river or region, with P values reported at the 5% significance level ($P < 0.05$) and indicated using an asterisk (*) if significant.

3.5.2. Quantile analysis

Flow duration curves were generated from daily discharge data to examine changes in quantiles. Daily ensemble-mean time series by decade were ranked, and the return period (between 1 day and 10 years, $n = 3,652$) was computed for the time series. Quantile plots were generated by plotting daily total discharge (log scale) for a river or region relative to the probability of nonexceedance (P) determined from an empirical cumulative distribution function generated by sorting these data using an R code.

3.5.3. Spectral analyses

Spectral analysis of discharge records was performed using simulated records (seven 30-year windows, averaged daily from January 1, 1981, to December 31, 2070, beginning at the start of each decade) for each of the 12 largest Arctic rivers and the three cluster regions (HBC_{REG}, HBC_{NOREG}, and Arctic). Analyses of periodicity were used to detect changes in time-series records at various frequencies, which distinguish hydropeaking from longer term, natural variability (Déry et al., 2018). Thirty-year time series underwent a windowed Fourier transform to derive spectral power for the periods of 2–365 days, with the goal to quantify the periodicity of the full hydrograph signal. As in Déry et al. (2018), a fitted curve (of the form $y = Ax^B$) was generated, where y is the spectral power, x is the period in days, and A and B are the fitted curve parameters, where B represents the slope of a straight line in log-log space. The slope (B) describes the variation in the strength of the periodicity from short windows (weekly hydropeaking) to longer windows (annual spring freshet). High slopes correspond to low periodicity at weekly scales and high periodicity at the annual scale typical of natural or unregulated rivers. Low slopes suggest strong weekly periodicity and/or weak annual periodicity typical of regulated rivers. Rivers with a strong freshet signal present the greatest power at the annual period, with harmonic spikes at fractional periods of 365 (i.e., 6 months, 3 months, 1.5 months). Although regulated rivers also present spikes in power at the annual timescale, their spectral power for lower return periods is noisier and stronger.

3.6. NEMO ocean modeling

For the BaySys project, the NEMO (Madec, 2008) version 3.6 numerical model was implemented across the ANHA domain at $\frac{1}{4}$ degree (approximately 15 km) resolution. Ridenour et al. (2019) presented the specific configuration of the model applied within the BaySys project, including a comparison between the more uniform (over time) input

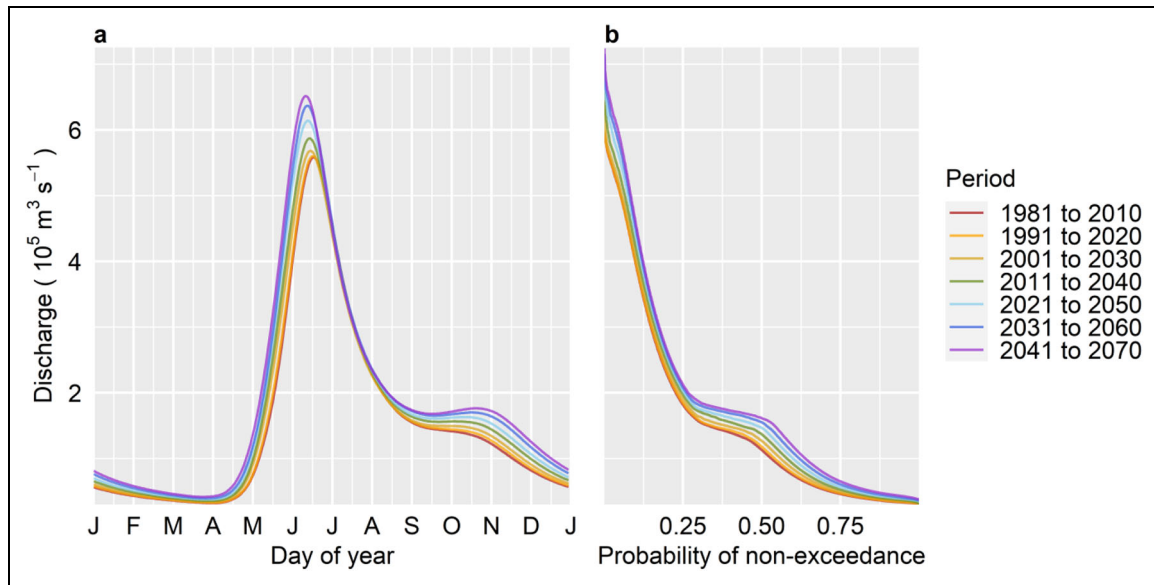


Figure 3. Average annual daily discharge and flow probability for all Arctic-draining rivers 1981–2070. Simulated ensemble mean (a) day-of-year average annual discharge by 30-year period and (b) empirically sorted flow duration curves by 30-year period ($n = 10,957$) for all pan-Arctic rivers (1981–2070). DOI: <https://doi.org/10.1525/elementa.2020.00098.f3>

from Dai and Trenberth, which covers only major rivers and not local runoff, relative to the HYPE-simulated runoff that is continuous over both time and space within the Hudson Bay domain.

Here, we compared A-HYPE modeled runoff to Dai and Trenberth because Dai and Trenberth is commonly applied in oceanographic studies. Further details on NEMO model specifics as established for the BaySys project are given in Ridenour et al. (2019), Dmitrenko et al. (2020), and Lukovich et al. (n.d.). Both experiments presented in this article were run for the period 2002–2009 with atmospheric forcing based on the ERA-Interim reanalysis, with all other model details equivalent. For simplicity, results are presented for the average of 2009 only, for regions with average salinity greater than 34.8 (i.e., the Atlantic Water) masked out.

4. Results

4.1. Trends in freshwater discharge to the Arctic Basin

When aggregating all Arctic-draining rivers and analyzing average annual daily discharge by decade, we detected a trend toward earlier and higher peak flows (Figure 3a). Differences among historic periods (1981–2020) are less than the differences projected among future periods (2021–2070) and are particularly notable in terms of the increasing peak discharge. A shift toward higher late fall and ice-on baseflow is notable, with differences among future periods being larger than historic. This shift suggests a trend toward earlier (and larger) spring melt events, delivering higher volumes of freshwater discharge to the Arctic earlier in the season than historically observed. Increasing spring freshet is coupled with wetter fall (low flow) periods, which are likely derived from increasing rainfall or rain on snow events caused by

a warmer climate. These changes can result in longer ice-free periods for Arctic-draining rivers and longer periods where rainfall can directly contribute to runoff within the pan-Arctic basins.

Flow duration curves reflect changes to the distribution of specific discharge values (y -axis) by plotting the probability of nonexceedance or chance of that discharge being equaled or exceeded (x -axis). Figure 3b reveals more significant increases to the more common (frequently occurring) lower quantile flows (probability of nonexceedance or $p > 50\%$) as a percentage increase of flow than to the median or higher quantile (large) events ($p < 25\%$). Warmer winter temperatures may increase water holding capacity of the atmosphere, resulting in more frequent winter precipitation events (Yang et al., 2016). Analyses of the climate scenarios over this region in our study reveal mean winter temperature increases of 2.5°C (Nelson Basin) to more than 6°C (Foxye Basin) by the 2070s, and corresponding winter precipitation increases exceeding 100 mm (East James Bay) in some regions (Table S3; Braun et al., n.d.). Particularly until the 2020s, less (relative) change in the annual freshet volume is anticipated (with larger changes noted in the far future), suggesting that more frequent winter snowfall events will not necessarily result in more snowpack accumulation. Although we see moderate increases to the highest quantile flows ($P < 10\%$), these are only as significant, if not less so, than the increases to low flow quantiles. The net result is a trend toward flattening of the average annual hydrograph (Figure 3b), where higher P values (low flows) are increasing at a faster rate than the lower P values (high flows), and therefore, seasonal differences in the volume of freshwater delivered to the Arctic are becoming less pronounced and more uniform (by volume) through time.

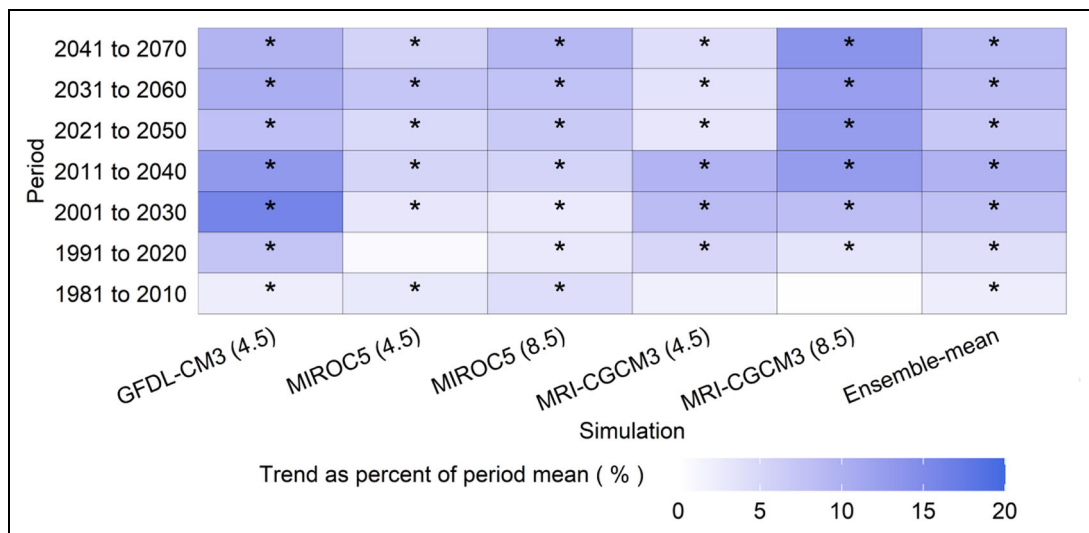


Figure 4. Thirty-year pan-Arctic discharge trends for ensemble members and ensemble mean. Sen’s slope from Mann–Kendall trend analysis in percentage of mean by 30-year periods by climate model for all Arctic basins. Simulation RCPs shown in parentheses. Members and periods with statistically significant (Mann–Kendall test, $P < 0.05$) trends are marked with (*). Ensemble mean is averaged daily across five GCM–RCP simulations. GCM = global climate model; RCP = representative concentration pathway. DOI: <https://doi.org/10.1525/elementa.2020.00098.f4>

Trends in freshwater discharge across the pan-Arctic domain revealed the same or slightly increasing discharge ($\text{m}^3 \text{s}^{-1}$ per decade), with statistically significant increases (indicated by asterisks) in future periods (Figure 4). No decreasing trends were projected, except under the influence of one GCM–RCP scenario (MIROC 5–RCP 4.5; Table 2) in one decade (2001–2010) that indicates a slight (statistically insignificant) decreasing trend. There is agreement among the results from all climate model projections in terms of both the direction and significance of discharge trends; all report statistically significant increasing trends for 30-year periods post-2020. Most of the climate scenarios (i.e., four of five) considered project an increase in the magnitude of the projected trend through time, as seen by darkening shades of blue in Figure 4. The last column of Figure 4 shows the ensemble mean, which exhibits a consistent and statistically significant increase (each period having an asterisk) from historic to future periods, which intensifies in magnitude (darkens) through time.

4.2. Temporal trends assessed across 90 years of record

The multidecadal periodicity analysis from Section 4.1 revealed evidence of an increasing trend in pan-Arctic discharge that appears to intensify into future periods, which is consistent with the literature (Durocher et al., 2019). Analysis of the continuous 90-year time series produced from all Arctic-draining rivers using Mann–Kendall trend revealed a statistically significant increasing trend over the record (Figure 5). Increasing freshwater discharge from the pan-Arctic rivers is particularly notable in future periods (2020–2070) relative to the historic trend (1981–2010), with an increase in slope visible around 2015. We report an increase of approximately $19 \text{ km}^3 \text{ yr}^{-1}$ over the 90-year constructed record, which

agrees in direction and magnitude with the $10 \text{ km}^3 \text{ yr}^{-1}$ rate reported from the historic trends for the six largest Eurasian rivers from 1936 to 2007 (Shiklomanov and Lammers, 2009), and with the increase of $8.7 \text{ km}^3 \text{ yr}^{-1}$ from 72 Arctic-draining rivers (1975–2015) reported by Durocher et al. (2019). Notable in our study, however, is the approximate doubling in the long-term trend that occurs by analyzing the full 90-year period, which includes a significantly wetter future period (2020–2070). According to this trend, we project up to a 22% increase in mean annual Arctic freshwater discharge (from 2011 to 2070).

Figure 5 similarly highlights an increase in the variability of discharge, or uncertainty, when moving from the historic to future periods of the 90-year record, where the future period is projected by the ensemble of GCM–RCP simulations considered in this study (i.e., from Table 2). There is significant uncertainty in the future freshwater discharge entering the Arctic system, which is being driven primarily by climate change. Variability in the historic period (1981–2020) represents input data uncertainty arising from the differences among historic climate (represented by HydroGFDv2) and that of the GCM–RCP ensemble (1981–2011), but of course is relatively smaller compared to the future period as a result of one truth for the historic period.

To better assess regional trends, we computed continuous time series of freshwater discharge for the 12 largest Arctic-draining rivers, applying Mann–Kendall trend analysis for each. All rivers show statistically significant increasing trends that vary in magnitude from $0.09 \text{ km}^3 \text{ yr}^{-1}$ (Koksoak, not including Caniapiscaw) to $2.6 \text{ km}^3 \text{ yr}^{-1}$ (Lena; Figure S2). The largest increases occur within the top four largest river basins by drainage area (in $\text{km}^3 \text{ yr}^{-1}$: Lena, 2.59; Yenisey, 2.48; Ob, 1.70; and Mackenzie, 1.60), which agrees with findings from Durocher et al. (2019)

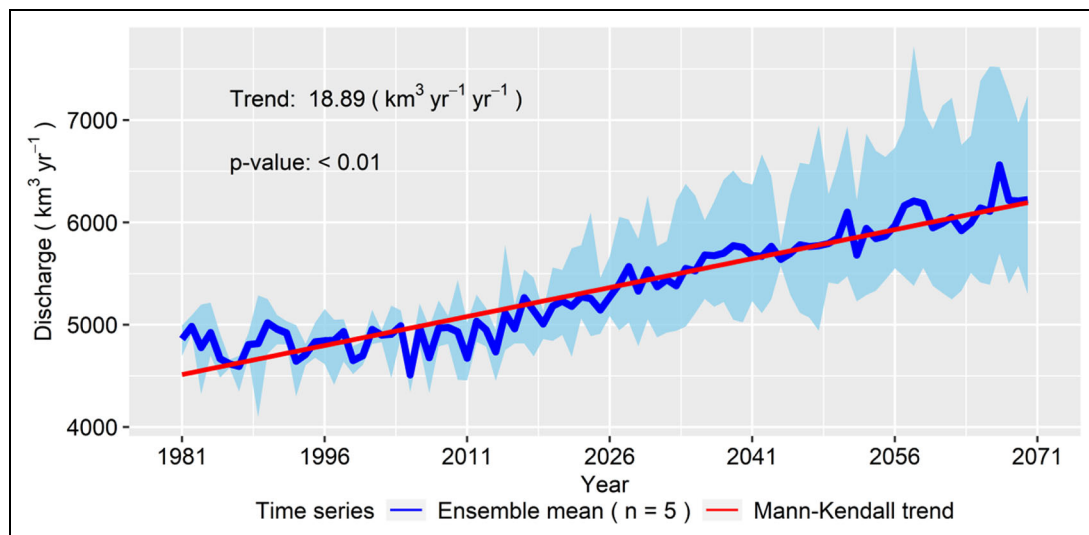


Figure 5. Modeled pan-Arctic annual discharge ensemble, ensemble mean, and Mann–Kendall trend and significance. Annual discharge from pan-Arctic watershed with Sen’s slope from Mann–Kendall trend analysis (1981–2070; red line), prewhitened by removing 1-year lagged autocorrelation prior to computing Mann–Kendall significance. Dark blue line represents the ensemble mean; light blue shading represents the ensemble range projected from hydrologic simulation of the five climate model inputs. DOI: <https://doi.org/10.1525/elementa.2020.00098.f5>

who reported larger increases in historically observed discharge originating from Eurasian Rivers. These increases point to evidence that warmer air temperatures are driving increasing precipitation, and subsequently runoff, as a proportion of drainage area, likely also supplemented with permafrost and frozen soil subsurface contributions. Significant upstream river (reservoir) regulation on the Yenisey will impact the rate of increase in future discharge observed at the outlet, which also explains the relatively flat trend in historical discharge (1981–2010; Figure S2d) in the observed record as the reservoir was filled (Shiklomanov and Lammers, 2009).

Statistically significant, but considerably smaller, increasing trends were detected within central and eastern North America, specifically for the Nelson, La Grande Rivière, and Koksoak Rivers (0.21, 0.21, and 0.10 km³ yr⁻¹, respectively; Figure S2h–j). These smaller increasing trends occur in rivers subject to significant diversion or regulation, which likely influences, or offsets, increasing climate-driven trends by partially decoupling the rainfall (or snowmelt) runoff response (Tefs, 2018).

4.3. Impact of river regulation on trends in freshwater discharge

To assess the impact of anthropogenic regulation on computed trends in freshwater discharge, we compared regulated and nonregulated rivers within a subregion of the pan-Arctic domain residing within the continental interior of Canada (Stadnyk et al., 2019). The HBC subregion was chosen because it lies within the pan-Arctic domain and is Arctic-draining, has known and described regulation on several of its largest rivers (i.e., Nelson and La Grande Rivière), and has been studied extensively within the BaySys project, including the modeling of regulation within this system (Tefs, 2018). Tefs (2018) demonstrated that up to $\pm 20\%$ seasonal variation in discharge could be

seen, mostly driven by climate change, within these HBC rivers (LGRC: -20% during summer, $+20\%$ during winter; NCRB: $+12\%$ in spring, -4% in autumn), amounting to a cumulative change of 1,100 m³ s⁻¹ average discharge (winter) of 7,800 m³ s⁻¹ total discharge, or approximately 7% of the total HBC inflow in the winter months (which see the most significant net change). The presence of regulation in a basin has the potential to impact, delay, or offset seasonal discharge even further (Déry et al., 2018).

To assess the relative impact of climate change and regulation on the HBC, we compared the time series for regulated and nonregulated rivers (Figure 6). Both systems project statistically significant ($P \ll 0.05$) increasing freshwater discharge into Hudson Bay, which is connected to the Arctic Basin via Foxe Channel and Fury and Hecla Strait. The reported increase for the regulated system, however, is approximately 30% less (0.76 km³ yr⁻¹) on average than that reported for rivers within the nonregulated system (1.14 km³ yr⁻¹). Given that the HBC, relative to the pan-Arctic domain, is smaller in expanse with comparatively representative (relative to the entire pan-Arctic domain) physiography and climatology, these differences can be attributed, at least in part, to the impact of river regulation (Déry et al., 2018). We compared the difference between renaturalized and regulated hydrologic simulations at 12 regulation points across the HBC by examining the trends of the 30-year ensemble means (Figure S3) and verify that renaturalized river regimes result in increased positive trends across historic and future time periods. Anthropogenic control of these rivers tends to damp long-term climate-driven trends, corroborating the findings of Déry et al. (2018) who report a damping of seasonal cyclicality in the average annual hydrograph due to river regulation. This damping agrees with findings that river regulation affects, more significantly than climate, freshwater discharge in Scandinavian Rivers (Arheimer et

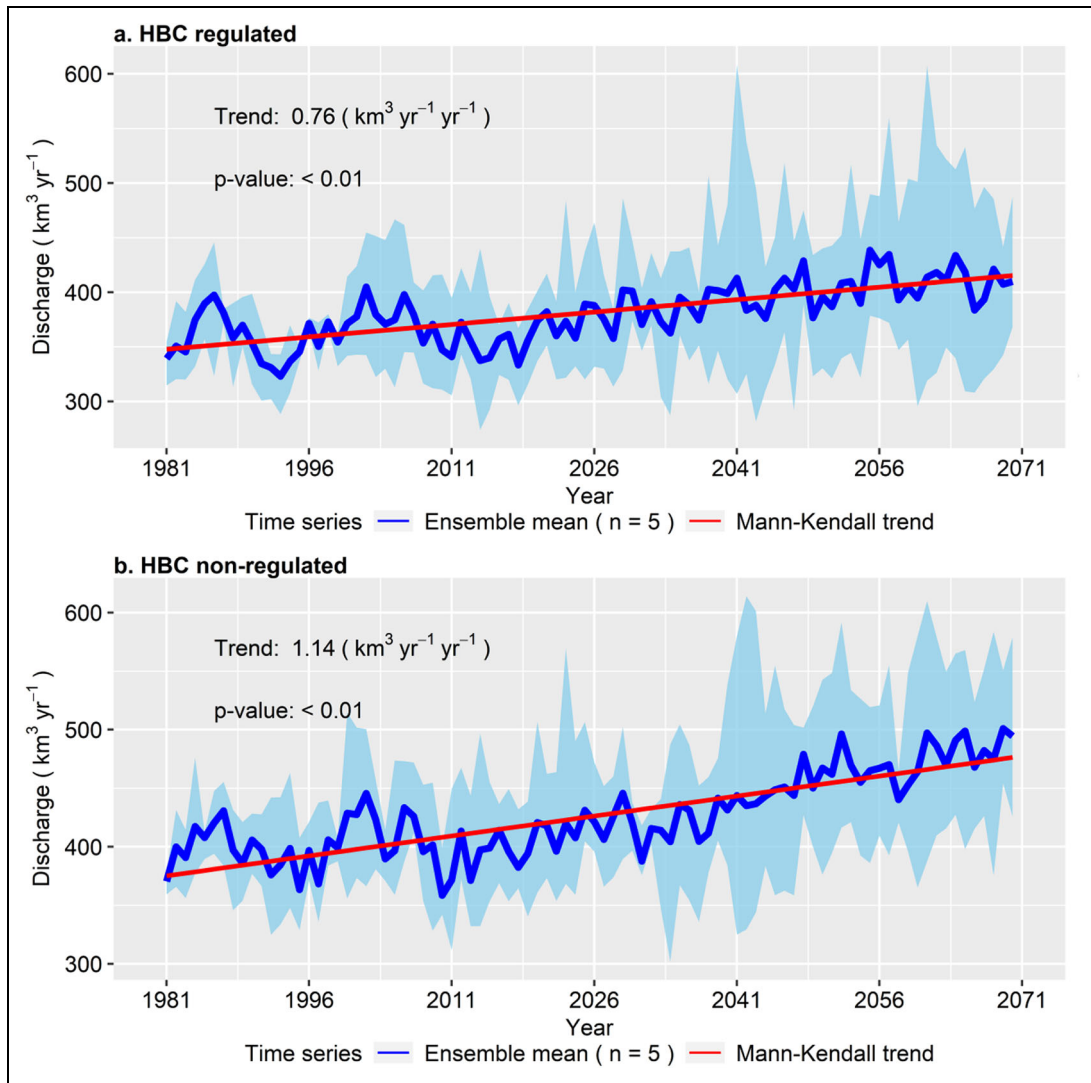


Figure 6. Modeled Hudson Bay annual discharge ensemble, ensemble mean, and Mann–Kendall trend and significance. Annual discharge from (a) regulated and (b) without regulation Hudson Bay Complex watersheds with Sen’s slope from Mann–Kendall trend analysis (1981–2070; red line), prewhitened by removing 1-year lagged autocorrelation prior to computing Mann–Kendall significance. Dark blue line represents the ensemble mean; light blue shading represents the ensemble range projected from hydrologic simulation of the five climate model inputs. DOI: <https://doi.org/10.1525/elementa.2020.00098.f6>

al., 2017). The considerable variability among the future climate simulations within this system, however, could alter the mean annual trend reported for both types of river systems. The presence of this (climatic) variability means that there could be little to no significant difference among the regulated and nonregulated systems in future periods (i.e., based on the upper and lower limits of the band in **Figure 6**).

Comparison of average annual hydrographs and flow duration curves for HBC_{REG} (Figure S4a and b) and HBC_{NOREG} (Figure S4c and d) systems clearly indicates the historic stepwise introduction of regulation, which was reported by Déry et al. (2018). In April, the La Grande reservoir levels rise rapidly in response to snowmelt but drop suddenly in mid-April, resulting in the sudden dip in the average annual regulated system hydrograph. In future periods, we assume no new development;

therefore, the uniformly distributed seasonal increases in discharge volume and flow quantiles are attributed to the regulation itself and the subsequent shift toward the more (economically desirable) uniformly distributed (in time) hydrograph. Uniformity in flow distribution is contrary to the natural cyclicality of the system, where climate change tends to increase lower quantile flows more substantially than the nival-dominated high flow quantiles (Figure S2d). A larger, secondary peak in late fall (November or December) seen in the regulated system (Figure S2a) becomes even more prominent in future periods. This prominence is likely the combined result of wetter fall/early winter conditions (also seen in Figure S2d) being exacerbated by increased hydropower production.

To further understand the impact of river regulation on this regime, we performed Mann–Kendall trend analyses by decade for each climate scenario (**Figure 7a**) and

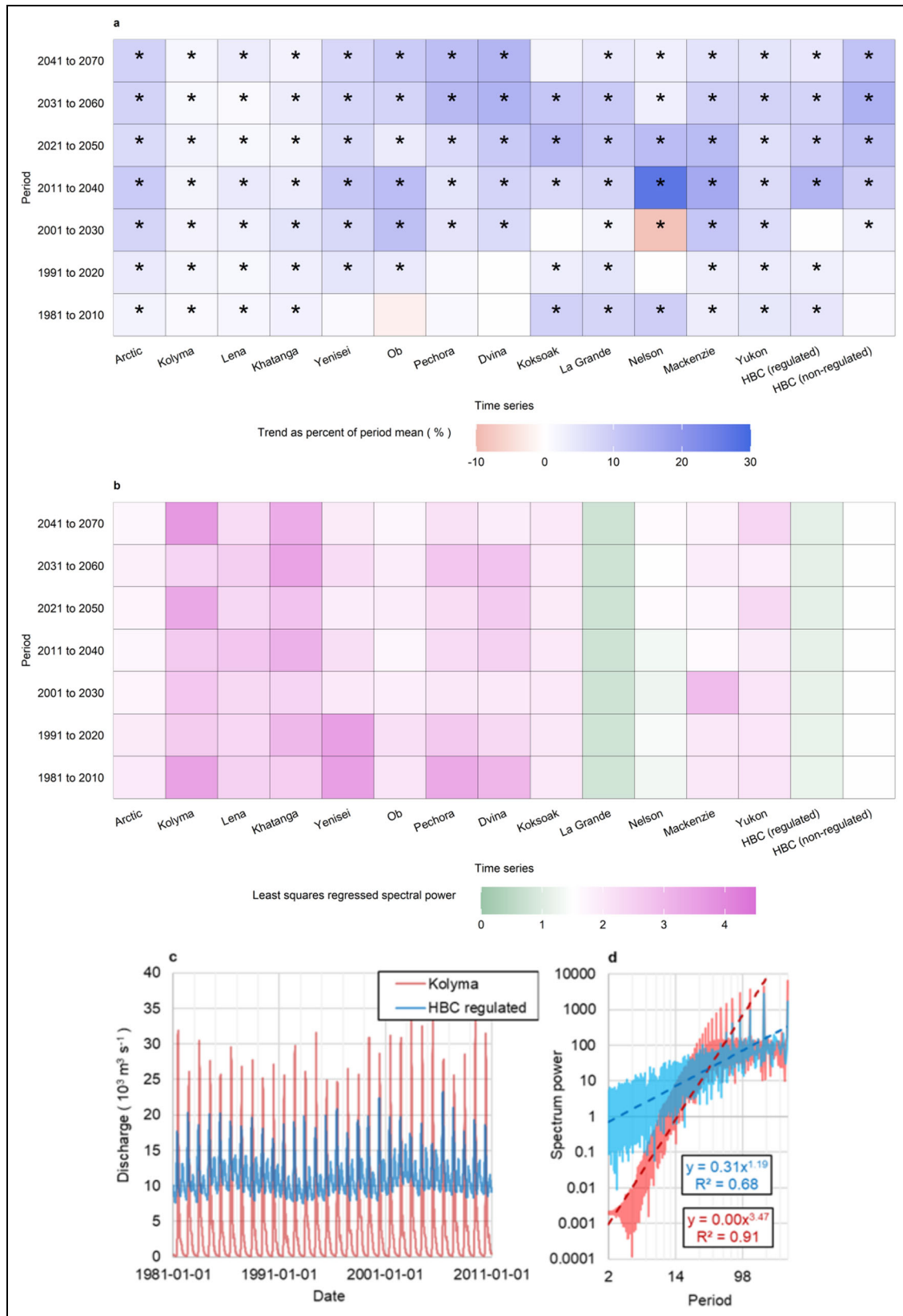


Figure 7. Ensemble-mean trend and slope of spectral analysis by river or region. Thirty-year analyses (1981–2070) for all Arctic-draining rivers and Hudson Bay Complex–regulated and nonregulated subregions for (a) normalized Sen’s slope of Mann–Kendall trend analysis (as percentage of period mean) and (b) slope of spectral power (B for $y = Ax^B$) of windowed Fourier transform analysis. Rivers ordered by longitude; asterisk (*) indicates statistical significance (Mann–Kendall test, $P < 0.05$). Example (c) 30-year daily time series (1981–2010) and derivation of (d) spectrum power and power function slope for two rivers, the Kolyma and HBC_{REG} (ensemble-mean), provided for illustration. DOI: <https://doi.org/10.1525/elementa.2020.00098.f7>

a windowed Fourier transform analysis on the HBC_{REG} and HBC_{NOREG} regimes (**Figure 7b**). For comparison, we plotted the results relative to those from the 12 largest pan-Arctic rivers, organizing the plot by longitude of the river outlet. The correlations of the final fitted power spectra by river and time period are provided in Table S2.

In the historic to near future periods (1981–2010 and 1991–2020), we observe offsetting east and west wet and dry periods across the pan-Arctic domain, with some statistically significant trends (indicated by asterisks; **Figure 7a**). For example, the 1981–2010 period appears to have been drier across Eurasia, while in North America, it was substantially wetter. In future periods, however, trends are far more consistent between the west and east, with increasing discharge evident among both Eurasian and North American rivers with near equal intensification (and significance). Intensification of the increasing trend is most apparent in the larger, nonregulated rivers within North America (e.g., Mackenzie, HBC_{NOREG}) but weaker in some larger unregulated Eurasian rivers (e.g., Lena). The Ob and Nelson Rivers are the only rivers to include decreasing (i.e., red) trends in one 30-year period each (only significant in the Nelson), both occurring within historic periods. Although the magnitude of increasing trends changes by period and river basin, all rivers and the Arctic basin overall report statistically significant increases from 2011 onward (**Figure 7a**).

River regulation within the HBC does not appear to affect the direction of change in freshwater discharge, with both the HBC_{REG} and HBC_{NOREG} systems in near exact agreement that freshwater discharge will increase into future periods (though not necessarily among individual GCMs; Figure S5). Differences in the significance of the slope trends across the 12 regulated rivers in the HBC were also limited; that is, only 46 instances where significance did not agree between regulated and renaturalized runs compared to 340 instances where both trend direction (sign) and significance were in agreement. In only 34 simulations, does the sign (direction of slope) of the trend change between renaturalized and regulated simulations. The magnitude of the annual slope trend, however, does change between regulated and renaturalized systems, with generally weaker increasing trends (smaller increases) exhibited in the regulated regimes. In Eurasian Rivers, specifically the Yenisey and Ob, reservoir infilling and the historic introduction of regulation reported by Shiklomanov and Lammers (2009) is detectable by the absence of any significant trend from 1981 to 2010 and a slight decreasing trend (insignificant) for the Ob (**Figure 7a**).

Comparing slopes of the spectral power in each basin from the windowed Fourier transform analysis (**Figure 7b**), we contrasted the periodicity of discharge within 30-year periods governed on shorter, weekly timescales (i.e., more likely to be regulated, lower spectral slope, green shades) versus those governed by the nival-dominated freshet period (i.e., monthly to annual timescales, higher spectral slope, or purple shades). As an example, we illustrate the relationship between the non-regulated Kolyma River (red) and HBC_{REG} system (blue)

time-series hydrographs (**Figure 7c**) and their subsequent power spectra derivations (**Figure 7d**). HBC_{REG} rivers have lower spectral slope than HBC_{NOREG} rivers, suggesting the presence of stronger weekly periodicity within the regulated basins, which is more typical of river regulation. La Grande Rivière, a highly regulated regime with a series of upstream reservoirs for hydropower generation, shows the lowest and most consistent periodicity among the 12 largest pan-Arctic Rivers; the Nelson River, also used for significant hydropower generation, similarly displays lower spectral slope with relative consistency.

Comparing the difference between individual renaturalized and regulated rivers by GCM simulation and time period (shown for the three largest regulated rivers in the HBC, which combined contribute more than 48% of average annual discharge by volume), we detected more significant positive trends (positive differences) than negative (Figure S5). Particularly evident in the La Grande and Nelson rivers is a pattern of increasing positive trends into future periods, suggesting greater differences between the renaturalized and regulated discharge regimes and a larger offset of the climate-driven increases in discharge as a result of river regulation.

These findings highlight the importance of considering river regulation within a hydrologic model setup, as the trend (and to a lesser extent significance or direction of trend) is evidently impacted, to some degree, by water management. Despite the significant river regulation in some Eurasian basins, the representation of regulation in Eurasian rivers was limited in this version of the model (i.e., only SMHI's seasonal regulation); hence, why Eurasian rivers present with higher overall spectral slope than the North American rivers (**Figure 7b**). The presence of a lower (relative to other Eurasian rivers) and more consistent shorter interval of periodicity in the flow record of the Ob and Yenisei Rivers is likely reflecting regulation (i.e., large upstream reservoirs).

Comparison between the nonregulated North American and Eurasian rivers demonstrates differences in the natural periodicity of freshwater discharge between continental systems (Mackenzie and Lena; **Figure 7b**), with North American rivers displaying lower spectral slope overall and more short-term variation in freshwater discharge. These findings could be attributed to the relative size of the basins (Lena is approximately 30% larger than the Mackenzie with nearly twice as much mean annual discharge), with North American rivers being characteristically smaller than the Eurasian rivers. Recent trends, however, may also point to significant increases in seasonal discharge from the large Eurasian Rivers, specifically the Lena, that are dominated by increasing spring freshet and decreasing summer and baseflow (Pohl et al., 2020), particularly evident after 2006 (Shiklomanov and Lammers, 2009). The relative differences in both the timing and magnitude of freshwater discharge from the North American and Eurasian continents are important considerations for the ocean thermohaline circulation, and the movement and extent of freshwater content plumes within the marine system.

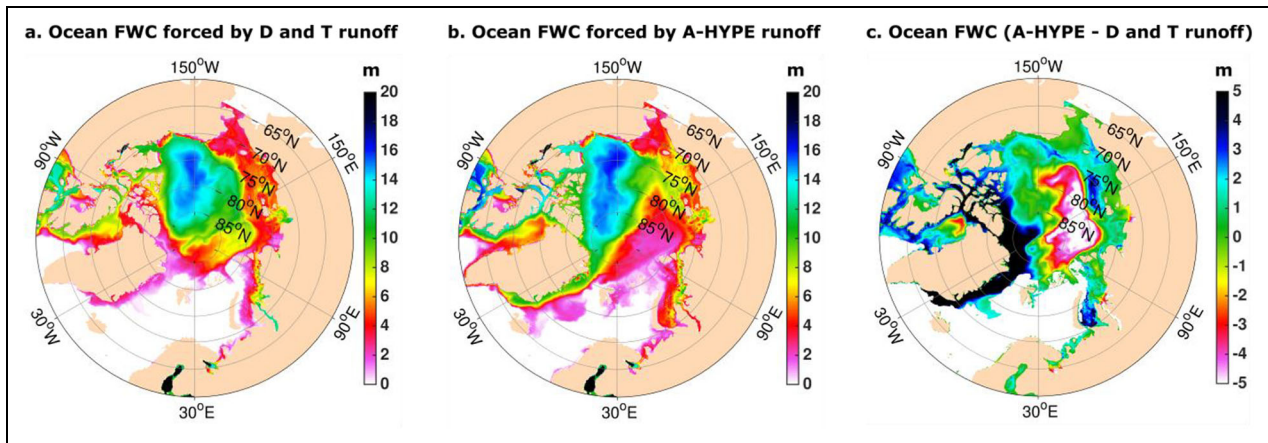


Figure 8. Nucleus for European Modelling of the Ocean simulated freshwater content in the Arctic Ocean, depth-integrated over the first 200 m. DOI: <https://doi.org/10.1525/elementa.2020.00098.f8>

4.4. Impact on Arctic Ocean salinity and freshwater content

We conducted a preliminary assessment of the impact of freshwater discharge on ocean salinity and freshwater content by comparing two versions of the NEMO model, forced with (a) Dai and Trenberth data commonly used in the marine community and (b) the long-term, more temporally and spatially continuous A-HYPE simulations. When the two versions of NEMO are compared across a shorter analysis period (2002–2009), important differences emerge when applying the A-HYPE forcing (**Figure 8**). First, higher freshwater content extends further eastward into the Lincoln Sea and the Greenland Sea (**Figure 8b**), which is closer to the observed pattern reported by Rabe et al. (2011) than in the simulation using Dai and Trenberth (**Figure 8a**). A wider high freshwater content band is also seen along the Siberian continental shelves under the A-HYPE forcing, suggestive of a stronger source or freshwater input. Strong freshwater content pathways from the Siberian shelves to the Beaufort Gyre are simulated using A-HYPE forcing that is not present under the Dai and Trenberth forcing. Morison et al. (2012) reported freshwater pathways most similar to those generated by the A-HYPE forcing, providing further evidence that the more continuous input of freshwater in time and space within this study generates results closer to observed salinity conditions over the long term.

A-HYPE simulations produced stronger and deeper freshwater content maximums in the Beaufort Gyre, and a freshwater content structure closer to the Alaskan coast, which has also been reported in observations (Proshutinsky et al., 2019). Maximum freshwater content at depth is underestimated relative to observations by A-HYPE, but Proshutinsky et al. (2019) focused their observations mostly on the summer periods. We generally find, and here report, that NEMO simulations of salinity and freshwater content forced by A-HYPE more closely match available observations relative to those generated under Dai and Trenberth forcing. Additionally, significantly fresher waters are exported from the Arctic through Fram Strait in the experiment forced by A-HYPE.

Vertically, A-HYPE simulations produced stronger and deeper freshwater content maxima in the Beaufort Gyre and a freshwater content structure closer to the Alaskan coast, which has also been reported in observations (Proshutinsky et al., 2019). Maximum freshwater content at depth is underestimated relative to observations by A-HYPE, but Proshutinsky et al. (2019) focused their observations mostly on the summer periods.

The resulting simulated distribution and amount of freshwater in the Arctic depends on the atmospheric forcing and the large-scale circulation; however, it also depends on the amount of freshwater being input and the seasonality and interannual variability of that input. Given that the two model experiments are twin experiments, with the NEMO same setup and identical atmospheric forcing, and that the only difference between the two experiments is the river runoff, this study demonstrates the importance and potential impact of the river runoff product used to drive an ocean model in determining the freshwater content of the Arctic Ocean. Future work is needed to analyze the detailed process-based changes, and, specifically, how the thermohaline circulation is impacted by different river runoff fields. Previous ocean modeling studies, such as those associated with the Forum on Arctic Modeling and Observational Synthesis, have shown the difficulty for the present generation of forced ocean general circulation models to get the Arctic freshwater content and transport correct (e.g., Ilicak et al., 2016; Wang et al., 2016). Those experiments used a common forcing field, including runoff based on Dai et al. (2009). Our results indicate that representation of river runoff may play an important role in setting the freshwater content structure in the Arctic Ocean and thus needs further study.

Freshwater content is calculated relative to a reference salinity of 34.8, averaged over 2009. Depth integration is over the top 200 m or up to the bathymetry for depths <200 m. Panel (a) is from the model forced by Dai and Trenberth and panel (b) is derived using A-HYPE for the pan-Arctic domain. Regions with freshwater content less than 0 m are masked (white). Panel (c) shows the

difference in freshwater content between the runs forced by A-HYPE minus Dai and Trenberth. Regions where the freshwater content is negative in either experiment are masked (white). The units for both panels are meters (m).

5. Discussion

5.1. Increasing freshwater discharge

Our results demonstrate that recent increases in pan-Arctic discharge are projected to continue into the future and will accelerate to a rate nearly twice that derived from historical data in the recent literature (Durocher et al., 2018; Pohl et al., 2020). An analysis of the 12 largest rivers (Figure S2) reveals no significant decreasing trend in any decadal period, indicating little to no likelihood of freshwater discharge decreasing in future periods. We can therefore anticipate more freshwater discharge entering the Arctic basin in future periods, hence higher freshwater content.

Previous work by Gelfan et al. (2017) compared two of the largest Arctic Rivers, one from North America (Mackenzie) and one from Eurasia (Lena). Although their reported mean changes in projected runoff were greater than we find for the Lena basin, the variability in projections (resulting from climate model input) was significantly higher for the Mackenzie Basin. They reported mean increases in average basin runoff from 5% to 19% for the Mackenzie basin and 10% to 25% for the Lena basin. In comparison, we project a 22% increase in pan-Arctic discharge, which is consistent (if not conservative) among previous studies for the pan-Arctic domain using climate model projections that report increases between 25% and 50% (Arnell, 2005; Van Vliet et al., 2011; Koirala et al., 2014; Bring et al., 2017). These previous projections, however, considered only portions of the full pan-Arctic domain and did not include river regulation.

Regionally, the most significant increasing trends occur in the Eurasian Rivers, which also correspond to the largest drainage areas, and therefore the largest discharge (historically, 1981–2010). When considering increasing projected discharge, summed from the largest four rivers (by volume) for Eurasia (Yenisey, Lena, Ob, and Dvina) and for North America (Mackenzie, Yukon, Nelson, and La Grande Rivière), then the projected relative increase for North America (0.93%) is 15% greater than that projected for Eurasia (0.79%; Table S1).

Interestingly, these results agree with the rates of change in freshwater content presented previously by Morison et al. (2012), observed for the period 2005–2008 using remote sensing imagery. They reported increases in freshwater content within the Canadian Basin of the Arctic Ocean that were countered at that time by decreasing Eurasian discharge. More recent studies focusing on Eurasian rivers have shown that since 2007, there have been notable increases in discharge from some of the largest Eurasian rivers (e.g., Lena and Yenisey rivers; Pohl et al., 2007; Shiklomanov and Lammers, 2009).

Results from the NEMO model using the A-HYPE forcing suggest even further propagation of freshwater content toward Greenland and the Labrador Sea than was reported by Morison et al. (2012). This finding warrants

further exploration of simultaneous, nonoffsetting increases in freshwater discharge from all continental landmasses entering the Arctic Ocean that may impact thermohaline circulation and the movement of freshwater (low salinity) plumes through the Arctic (marine) Basin. This study provides clear evidence that such increases will impact ocean salinity and freshwater content, and likely global oceanic circulation, but does not yet resolve the magnitude or extent of those impacts. Differential increases in freshwater discharge from the continents, or strongly additive freshwater exports, potentially exert an additional driving force on global ocean circulation patterns, sea ice production, movement, and breakup.

5.2. Changing seasonality

The most significant shift in the pan-Arctic average annual hydrograph occurs in the lower quantile low, or recession limb, flows that are more typical of late fall and winter (ice-on) periods (Figure 3b). This shift can have significant implications for the Arctic region in future periods, given that historically several of these rivers have frozen to the bed for 5 or more months of the year. Rennermalm et al. (2010) also reported increasing cold season low flows over most of the pan-Arctic domain, and in particular, the Eurasian basins. They reported similar increases, though to a lesser extent, for the Mackenzie basin and a decreasing trend in low flow across Eastern Canada (i.e., Nelson and southern Hudson Bay regions) in the late 20th century. They pointed to significant discrepancy within the literature on the direction of trends within the Canadian basins and to a lack of observations and incongruent temporal periods of analysis as the cause. We found a weak (insignificant) decreasing trend or no trend in total discharge across Eurasia from 1981 to 2010 (Figure 7a). This finding, however, was followed in our 30-year moving-window analysis by significant increasing trends by 2001–2030, with ubiquitous increasing trends in all rivers by the 2011–2040 period. Examination of the flow duration curves (Figure S4d) for Eastern Canada, the HBC_{NOREG} system, shows tight clustering of low (and high) flow quantiles throughout much of the historic period and in the near future, but a distinct shift toward higher low flow quantiles post-2030. Flow duration curves within the regulated system are more uniformly distributed by decade, which is likely an artifact of water management practices in regulated rivers (Figure 3b).

Increasing cold season low flows are likely the result of increasing autumn rain events and winter rain on snow events (due to warmer air masses), resulting in later onset of ice cover and a shorter snow cover season. This scenario, coupled with an earlier spring melt, reduces the total duration of ice cover forming on Arctic-draining rivers, which has significant implications for Arctic transportation and mobility (Pizzolato et al., 2014; Scheepers et al., 2018), as well as ecosystem processes. A shorter cold season will increase thawing of permafrost and frozen ground, subsequently increasing soil moisture storage and therefore runoff ratios. Changing amounts of subsurface storage are thought to be the main driver behind late 20th century changes in freshwater discharge to the Arctic

(Rennermalm et al., 2010). Changes in subsurface storage will also impact the risk of severe drought or forest fire in the pan-Arctic domain (Groisman et al., 2007), destabilizing soil structures and influencing surface water accumulation and runoff (Smith et al., 2005), altering species composition and influencing landcover (Baltzer et al., 2014; Jafarov et al., 2018), and affecting the physical properties and nutrient composition of river discharge into the marine system (Pozdnyakov et al., 2007; Semiletov et al., 2011).

Spring peak flows produced by a single, spring pulse of snowmelt have similarly increased in recent decades and are projected to further increase into the future (**Figure 3a**), although not as significantly as the increases in the lower regime flows (**Figure 3b**). These spring increases contribute to a general and gradual flattening of the average annual hydrograph or a more uniform (in time) delivery of freshwater to the Arctic (marine) Basin as opposed to the traditional freshwater “pulse” in spring. This effect is similar to the reported impact of regulation on the average annual hydrograph (Arheimer et al., 2017; Déry et al., 2018), which further complicates discharge and trend projection. Shifting toward a more uniform seasonal delivery of freshwater into the marine system is likely to have significant biogeochemical implications, impacting species health and biodiversity, particularly on continental shelves influenced by the halocline (Prowse et al., 2006).

5.3. Influence of river regulation

Our analysis within the HBC subdomain suggests that regulation exacerbates climate-driven impacts, contributing to a further flattening of the average annual hydrograph and more uniform delivery of freshwater into the Arctic Basin. By contrasting regulated and nonregulated systems within comparatively representative (relative to the rest of the pan-Arctic domain) physiographic and climatological regions, we first see the gradual, stepwise introduction of river regulation within the system differentiated by decades, as also noted by Déry et al. (2018). Second, we detect the presence of a more significant dual-peak in the regulated system (rising in late fall, peaking in winter) due to wetter fall conditions (Figure S4a and c).

In this work, we find climate-driven and anthropogenic effects to be offset by river regulation, on average. This finding is important because offsetting effects complicate the separation of anthropogenic and climate-driven signals within discharge records as the trends and their significance tend to be lower. Trend analysis reveals that river regulation reduces the likelihood of detecting a significant increasing trend within similar physiographic and climatic regions (**Figure 7a**). We hypothesize that significant inter-annual storage in systems (e.g., the LGRC) could be due to retention of peak annual flows across multiple years. The reduced likelihood of detecting an increasing trend may also be an artifact of the increased 7-day coefficient of variation in regulated flow systems (Déry et al. 2018), which may damp the magnitude of detected trends because of both natural persistence and nonstationarity introduced by the presence (and gradual introduction over time) of flow regulation (Bayazit, 2015). The identification

of different long-term trends for the HBC_{REG} and HBC_{NOREG} regimes demonstrates the importance of considering anthropogenic influences, like river regulation, at the continental scale when producing climate change scenarios, likely necessitating more complex integrated water resource management models to assess long-term trends accurately. In many continental-scale projections, such anthropogenic influence is ignored in place of examining climate-driven change, which may result in misleading trend identification.

Changes in water availability, however, influence the storage and release of water in large river systems, ultimately impacting both the timing and delivery of freshwater volume to the Arctic Ocean or downstream system. Although the timestep of flow and reservoir operating decisions may occur in some reservoirs on a daily or weekly timescale (i.e., hydropeaking), we find that regulation decisions in the large, Arctic-draining rivers can influence monthly and annual cumulative downstream freshwater discharge. Given that the timing of freshwater delivery is important for the Arctic benthic and pelagic ecosystems (Sibert et al., 2010; Castro de la Guardia et al., 2019), ensuring that models adequately account for anthropogenic controls on continental freshwater discharge is also important.

The use of spectral analyses and windowed Fourier transforms identified the periodicity of the largest Arctic-draining rivers and subregions (**Figure 7b**), highlighting the importance (and dominance) of the spring freshet within these systems. Important timing differences among the North American and Eurasian river regimes (independent of regulation) were also identified, suggesting higher natural intraannual variability in the Eurasian rivers. The dominance of a single, nival-driven peak flow event is less obvious among North American regimes. In western Canada (Mackenzie and Yukon rivers), snowmelt peaks contribute to higher (than eastern Canada) spectral slope (**Figure 7b**), suggesting dominant monthly to annual timescale events. Spectral slopes, however, are lower and less consistent than those from Eurasian rivers, suggesting the increasing dominance of rainfall-dominated events interspersed throughout the year. Eastern Canadian rivers exhibit lower spectral slope, suggesting the dominance of higher frequency events (weekly to monthly timescale) that likely are a combination of regulation and lower-latitude drainage from more temperate climates.

The significance of uncertainty in these simulations, particularly for the regulated and nonregulated system comparison, is important. If upper and lower bounds of this assessment are considered, then a much greater (lesser) increasing (decreasing) trend would be reported (**Figure 6a and b**). The presence of regulation within a river regime will increase uncertainty in reality (though this uncertainty will not necessarily be accounted for in simulation), resulting from unknown unknowns (Klemeš, 1997)—we cannot predict, with certainty, how water management rules will be adapted into the future to compensate for changing climates and water supply. Similarly, regulated system analyses here do not account for future

infrastructure that is under construction or could be built within large Arctic drainage basins, though our analysis suggests that hydropower potential will likely increase in the future. Whether or not new infrastructure will be developed depends on a multitude of factors, including (but not limited to) the economics of such projects, the energy landscape, and future legislation and policy, all of which are difficult to forecast and would require more sophisticated integrated water resource management models. Unfortunately, such a comprehensive model is not yet computationally feasible for the entire pan-Arctic domain.

Even among the known unknowns (i.e., input, parameter, and model structural uncertainty), there is the issue of uncertainty propagation through the modeling chain to arrive at a cumulative estimate of downstream (outlet) uncertainty for projected discharge (Pokorny et al., 2021). This issue presents a specific challenge for high-latitude basins, such as the pan-Arctic domain, where data are sparse and the region is highly diverse and complex hydrologically, requiring a relaxation of normally more stringent model calibration guidelines. This relaxation, of course, has implications for the accuracy with which we can expect to predict continental-scale freshwater discharge, and the extent to which we trust hydrometric measurement in complex, cold region (ice-affected) regimes (Hamilton and Moore, 2013; Westerberg et al., 2020). We suggest that more sensitivity experiments, including the uncertainty associated with using a single hydrologic model structure, are needed to ascertain the cumulative impact of discharge uncertainty and variance on downstream marine systems.

5.4. Impacts to the marine system

Our analysis with the NEMO model was a first attempt at utilizing continuous (in time and space) freshwater discharge as input to an ocean model used for climate purposes, and our results demonstrate the impact of freshwater discharge on the marine system. Previous ocean model simulations generally relied on long-term, gap-filled records such as Dai and Trenberth (Dai et al., 2009) in the absence of continental or global-scale freshwater discharge. We show that subtle differences in the timing and magnitude of freshwater forcing in ocean models can culminate in significant differences in localized salinity and freshwater content and the extent to which freshwater plumes spread across the Arctic Basin.

The AMOC, critical for Earth's climate and the distribution of heat and carbon, has been reported as weakening in recent decades (Caesar et al., 2018). Increasing freshwater discharge into the Arctic Basin and the melting of the Greenland ice sheet have been suggested as contributing to a weakening of the Labrador current and the AMOC (Thornalley et al., 2018). As terrestrial freshwater discharge volumes are changing seasonally, so too is the temperature of these freshwater fluxes. This change, in turn, can impact sea surface temperature and the formation and breakup of sea ice within the Arctic Ocean. Understanding the complex linkages between the weakening AMOC and increasing freshwater discharge is therefore crucial for

disentangling feedback mechanisms between the ocean, changes in the terrestrial system, and future climate and weather extremes.

Increasing freshwater discharge has a significant impact on the primary productivity of the Arctic Basin, as increasing discharge reduces nutrient availability through an intensified stratification in the water column. This impact is offset, however, by increasing light availability due to loss of sea ice, particularly during warmer summer seasons. In Hudson Bay, for example, increased ice-free seasonality, coupled with strong wind turbulence, results in higher primary productivity for Hudson Bay, yet is not the case for the Canadian Arctic Archipelago, Baffin Bay, or Beaufort Gyre (Castro de la Guardia et al., 2019). These conflicting results highlight how little is known about the connectivity between climate-driven changes to sea ice, the role of freshwater discharge, and the net impact on primary productivity of the marine system.

The fundamental need for more diverse and spatially distributed data to support modeling efforts within the pan-Arctic region, and for the detection and diagnosis of climate-driven change, is clear (Tang et al., 2020). The emergence of remote sensing data, and their acquisition at higher latitudes, has greatly improved knowledge of the Arctic Basin, but their time series is relatively short with availability limited to contemporary periods. Their applicability for paleo or future trend projection is thus limited. Therefore, equally as important, is the need for coupled Earth System Models to link climate, hydrologic, and marine systems to enhance our understanding of cumulative system impact and feedback mechanisms between the systems.

6. Conclusions

Using a model calibrated to historical Arctic-HYCOS records, we project discharge across the pan-Arctic basin to derive a more temporally and spatially continuous 90-year record of freshwater discharge entering the Arctic Basin. We find that freshwater discharge is increasing significantly for all rivers, with a projected 22% overall increase in discharge to the Arctic Basin that is more uniform (than in the past) across both Eurasia and North America. Despite the rate of increase being greater among Eurasian rivers, we find a slightly larger percent increase in North American freshwater contribution. Differential changes in Eurasian and North American discharge may have significant implications for future Arctic Ocean circulation and salinity distribution.

Both climate change and river regulation are contributing to a flattening of the average annual hydrograph. This flattening is partly due to statistically significant increases in lower quantile flows (late fall and winter recession) and partly driven by the onset of an earlier and comparatively smaller increase in spring freshets. The latter contribute to decreasing seasonality and a more uniform delivery of freshwater discharge into the Arctic Basin, which can have significant implications for the continental shelves and their ecosystems. Increasing anthropogenic river regulation has intra-annual impacts similar to climate change by simultaneously contributing to additional

flattening of the hydrograph. Spectral analyses distinguished between climate-driven and higher frequency hydropeaking signals; however, this distinction was only possible when simulating (weekly or monthly) river regulation or water management practices in the modeled scenarios. This result highlights the need to embed river regulation for pan-Arctic rivers within hydrologic models to generate more representative time series of discharge, historical, and future.

When A-HYPE discharge was used to force the NEMO ocean circulation model, increased freshwater content associated with regions of increasing river discharge is evident. This study and others within the BaySys project provide evidence that dynamic discharge (continuous in time and space and changing over time in response to climate), relative to static (long-term mean) inputs, may influence long-term oceanic circulation (Ridenour et al., 2019) and hence will likely impact projections of sea ice and biogeochemical processes. Such impacts are important to note for the ocean modeling community as they indicate that continued use of products based on long-term mean discharge (like Dai and Trenberth) for future simulations will likely be insufficient, particularly with the significant increases and spatial variability shown among future projections.

The hydrologic modeling conducted within this study did not consider nonstationarity under future climate directly and instead used historic (current) landcover distributions to derive model parameters, which were held constant over the simulation period. Rubel and Kottek (2010) show that landcover classifications (reported using KPn) may undergo significant change, particularly in the higher latitude regions of the planet. This change will impact landcover distribution, and hence model parameterization, and potentially have a significant impact on runoff-generating processes. Therefore, future modeling exercises should account more realistically for nonstationarity in landcover under climate-driven change to examine the redistribution of runoff and therefore future discharge.

Although this work presents a first, important step in modeling the pan-Arctic domain, it represents only a fraction of what is needed. A critical need is to provide runoff data in ungauged areas of the pan-Arctic domain, like the Canadian Arctic Archipelago where there are no gauges and therefore no records of climate impacts. These high-latitude regions, where gauging is at its lowest density, represent some of the most impacted regions of the world, and hence documenting climate-induced hydrologic impacts using coupled modeling approaches is crucial for improving knowledge in ungauged regions (Bring and Destouni, 2011). The potential offered by remote sensing products and applications across the polar region (Tang et al., 2020) should also be explored to assist with validating and verifying model outcomes (discharge) and process-based hydrologic estimates (e.g., evapotranspiration and snow-water equivalent). Future work must include Greenland freshwater discharge; the freshwater discharge from Greenland (estimated at $280 \pm 58 \text{ km}^3 \text{ yr}^{-1}$ by Velicogna et al., 2014) now potentially rivals that of the Mackenzie

River basin and hence could have a significant impact on the freshwater content and salinity of the North Atlantic (Scheepers et al., 2018; Stroeve and Notz, 2018) and on thermohaline circulation originating in the Arctic Ocean. Future applications of the coupled NEMO-AHYPE simulation system will include Greenland within the terrestrial domain and consider Greenland freshwater discharge in ocean freshwater content simulations.

Data accessibility statement

The Fortran code used to carry out the Nucleus for European Modelling of the Ocean (NEMO) simulations can be accessed from the NEMO version 3.6 repository (<https://forge.ipsl.jussieu.fr/nemo/browser/NEMO/releases/release-3.6>, last access: 14 October 2020). The initial and boundary conditions, atmospheric forcing, and numerical output were too large to host on a repository and are instead hosted on our lab's servers as well as the Compute Canada Graham system (<http://www.computecanada.ca>). Freshwater discharge runs for Hudson Bay domain are available here and historic discharge for the pan-Arctic domain from SMHI HYPEweb (<https://hypeweb.smhi.se/explore-water/historical-data/arctic-long-term-means/>). Future runs under the five specific climate simulations used in this study are available upon request, with a high and low resolution output available on the HYPEweb (<https://hypeweb.smhi.se/explore-water/climate-change-data/arctic-climate-change/>).

Supplemental files

The supplemental files for this article can be found as follows:

Table S1. Validation results for all pan-Arctic rivers, summarized by region (bolded), as simulated by the revised Arctic-Hydrological Predictions for the Environment model.

Table S2. Correlation (R^2) between computed spectral power (2–365 days) and fitted spectral power curve.

Table S3. Change in winter temperature and precipitation in near and far future periods for Hudson Bay subregions.

Figure S1. Modeled performance of monthly discharge of 74 pan-Arctic gauges.

Figure S2. Modeled pan-Arctic annual discharge ensemble, ensemble mean, and Mann-Kendall trend and significance.

Figure S3. Ensemble mean of trend differences [$|$ Renaturalized $|$ – $|$ Regulated $|$].

Figure S4. Average annual daily discharge and flow probability for the period 1981–2070.

Figure S5. Trends by time period and global climate model for regulated and renaturalized configurations.

Acknowledgments

The authors would like to thank the Nucleus for European Modelling of the Ocean (NEMO) development team as well as the DRAKKAR group for providing the model code and continuous guidance. They thank their project partners and industrial team leads, Kristina Koenig and Kevin Gawne (Manitoba Hydro) and Catherine Guay (Hydro-

Québec), for their helpful advice and feedback throughout this work. They thank Marco Braun (Ouranos) for providing the downscaled climate data required to perform model simulations over the pan-Arctic domain. Berit Arheimer and those at the Swedish Meteorological and Hydrological Institute provided the foundational Arctic-Hydrological Predictions for the Environment hydrological code and the input forcing data (HydroGFDv2). They also acknowledge the contributions of Rodell Salonga who produced the first version of some of these trends as a summer student in the UC-HAL. They thank the reviewers whose detailed comments and suggestions along the way (including two anonymous referees) helped to greatly improve this article.

Funding

This research was funded by the Natural Sciences and Engineering Research Council (NSERC) of Canada, a national granting agency. Research was conducted as part of the BaySys collaborative research and development NSERC grant (D. Barber), which was jointly supported by Manitoba Hydro (cash contribution) and the following agencies: ArcticNet, Ouranos, Hydro-Québec, and various Canadian Universities (in-kind).

Competing interests

The authors declare that there are no competing interests or conflict of interest with this research or the preparation and submission of this article.

Author contributions

- Contributed to conception and design: MB, TAS, SJD, DG, KK.
- Contributed to acquisition of data: MB, AT, SJD, DG, KK.
- Contributed to analysis and interpretation of data: TAS, SJD, MB, AT, PGM, NR, KK.
- Drafted and/or revised this article: TAS, AT, MB, PGM, NR, LV, SJD, DG, KK.
- Approved the submitted version for publication: TAS, AT, MB, PGM, NR, LV, SJD, DG, KK.

References

- Aagaard, K, Carmack, EC.** 1989. The role of sea ice and other fresh water in the Arctic circulation. *Journal of Geophysical Research: Oceans* **94**(C10): 485–498. DOI: <http://dx.doi.org/10.1021/jp0010379>.
- Andersson, J, Pechlivanidis, I, Gustafsson, D, Donnelly, C, Arheimer, B.** 2015. Key factors for improving large-scale hydrological model performance. *European Water* **49**: 77–88.
- Arheimer, B, Donnelly, C, Lindström, G.** 2017. Regulation of snow-fed rivers affects flow regimes more than climate change. *Nature communications* **8**(1): 1–9. DOI: <http://dx.doi.org/10.1038/s41467-017-00092-8>.
- Arheimer, B, Lindström, G.** 2014. Electricity vs Ecosystems-understanding and predicting hydro-power impact on Swedish river flow. *Proceedings of the International Association of Hydrological Sciences* **364**: 313–319. DOI: <http://dx.doi.org/10.5194/piahs-364-313-2014>.
- Arheimer, B, Pimentel, R, Isberg, K, Crochemore, L, Andersson, JCM, Hasan, A, Pineda, L.** 2020. Global catchment modelling using World-Wide HYPE (WWH), open data, and stepwise parameter estimation. *Hydrology and Earth System Sciences* **24**(2): 535–559. DOI: <http://dx.doi.org/10.5194/hess-24-535-2020>.
- Arnell, NW.** 2005. Implications of climate change for freshwater inflows to the Arctic Ocean. *Journal of Geophysical Research: Atmospheres* **110**(D7): D07105. DOI: <http://dx.doi.org/10.1029/2004JD005348>.
- Baltzer, JL, Veness, T, Chasmer, LE, Sniderhan, AE, Quinton, WL.** 2014. Forests on thawing permafrost: Fragmentation, edge effects, and net forest loss. *Global Change Biology* **20**(3): 824–834. DOI: <http://dx.doi.org/10.1111/gcb.12349>.
- Bamber, JL, Tedstone, AJ, King, MD, Howat, IM, Enderlin, EM, van den Broeke, MR, Noel, B.** 2018. Land Ice Freshwater Budget of the Arctic and North Atlantic Oceans: 1. Data, Methods, and Results. *Journal of Geophysical Research: Oceans* **123**(3): 1827–1837. DOI: <http://dx.doi.org/10.1002/2017JC013605>.
- Bamber, JL, Van Den Broeke, M, Ettema, J, Lenaerts, J, Rignot, E.** 2012. Recent large increases in freshwater fluxes from Greenland into the North Atlantic. *Geophysical Research Letters* **39**(19). DOI: <http://dx.doi.org/10.1029/2012GL052552>.
- Bayazit, M.** 2015. Nonstationarity of hydrological records and recent trends in trend analysis: A state-of-the-art review. *Environmental Processes* **2**(3): 527–542. DOI: <http://dx.doi.org/10.1007/s40710-015-0081-7>.
- Berg, P, Donnelly, C, Gustafsson, D.** 2018. Near-real-time adjusted reanalysis forcing data for hydrology. *Hydrology and Earth System Sciences* **22**(2): 989–1000.
- Braun, M, Thiombiano, A, Vieiria, M, Stadnyk, TA.** n.d. Representing climate evolution in ensembles of GCM simulations for the Hudson Bay system. *Elementa: Sciences of the Anthropocene* (submitted: ELEMENTA-S-21-00009)
- Bring, A, Destouni, G.** 2011. Relevance of hydro-climatic change projection and monitoring for assessment of water cycle changes in the Arctic. *Ambio* **40**(4): 361–369. DOI: <http://dx.doi.org/10.1007/s13280-010-0109-1>.
- Bring, A, Shiklomanov, A, Lammers, RB.** 2017. Pan-Arctic river discharge: Prioritizing monitoring of future climate change hot spots. *Earth's Future* **5**(1): 72–92. DOI: <http://dx.doi.org/10.1002/2016EF000434>.
- Burn, DH, Hag Elnur, MA.** 2002. Detection of hydrologic trends and variability. *Journal of Hydrology* **255**

- (1–4): 107–122. DOI: [http://dx.doi.org/10.1016/S0022-1694\(01\)00514-5](http://dx.doi.org/10.1016/S0022-1694(01)00514-5).
- Caesar, L, Rahmstorf, S, Robinson, A, Feulner, G.** 2018. Observed fingerprint of a weakening Atlantic Ocean overturning circulation. *Nature* **556**(7700): 191–196.
- Carmack, E, Winsor, P, Williams, W.** 2015. The contiguous pan-Arctic riverine coastal domain: A unifying concept. *Progress in Oceanography* **139**: 13–23. DOI: <http://dx.doi.org/10.1016/j.pocean.2015.07.014>.
- Castro de la Guardia, L, Garcia-Quintana, Y, Claret, M, Hu, X, Galbraith, ED, Myers, PG.** 2019. Assessing the role of high-frequency winds and sea ice loss on Arctic phytoplankton blooms in an ice-ocean-bio-geochemical model. *Journal of Geophysical Research: Biogeosciences* **124**(9): 2728–2750. DOI: <http://dx.doi.org/10.1029/2018JG004869>.
- Chen, J, Brissette, FP, Chaumont, D, Braun, M.** 2013. Finding appropriate bias correction methods in downscaling precipitation for hydrologic impact studies over North America. *Water Resources Research* **49**(7): 4187–4205. DOI: <http://dx.doi.org/10.1002/wrcr.20331>.
- Curry, R, Mauritzen, C.** 2005. Dilution of the northern North Atlantic Ocean in recent decades. *Science* **308**(5729): 1772–1774. DOI: <http://dx.doi.org/10.1126/science.1109477>.
- Dai, A.** 2017. Dai and Trenberth global river flow and continental discharge dataset. *Data archive at the national center for atmospheric research, computational and information systems laboratory*. DOI: <http://dx.doi.org/10.5065/D6V69H1T>.
- Dai, A, Qian, T, Trenberth, KE, Milliman, JD.** 2009. Changes in continental freshwater discharge from 1948 to 2004. *Journal of Climate* **22**(10): 2773–2792. DOI: <http://dx.doi.org/10.1175/2008JCLI2592.1>.
- Déry, SJ, Hernández-Henríquez, MA, Burford, JE, Wood, EF.** 2009. Observational evidence of an intensifying hydrological cycle in northern Canada. *Geophysical Research Letters* **36**(13). DOI: <http://dx.doi.org/10.1029/2009GL038852>.
- Déry, SJ, Mlynowski, TJ, Hernández-Henríquez, MA, Straneo, F.** 2011. Interannual variability and interdecadal trends in Hudson Bay streamflow. *Journal of Marine Systems* **88**(3): 341–351. DOI: <http://dx.doi.org/10.1016/j.jmarsys.2010.12.002>.
- Déry, SJ, Stadnyk, TA, MacDonald, MK, Gaulti-Sharma, B.** 2016. Recent trends and variability in river discharge across northern Canada. *Hydrology and Earth System Sciences* **20**(12). DOI: <http://dx.doi.org/10.5194/hess-20-4801-2016>.
- Déry, SJ, Stadnyk, TA, MacDonald, MK, Koenig, KA, Guay, C.** 2018. Flow alteration impacts on Hudson Bay river discharge. *Hydrological Processes* **32**(24). DOI: <http://dx.doi.org/10.1002/hyp.13285>.
- Dickson, RR, Meincke, J, Malmberg, SA, Lee, AJ.** 1988. The “great salinity anomaly” in the Northern North Atlantic 1968–1982. *Progress in Oceanography* **20**(2): 103–151. DOI: [http://dx.doi.org/10.1016/0079-6611\(88\)90049-3](http://dx.doi.org/10.1016/0079-6611(88)90049-3).
- Dmitrenko, IA, Myers, PG, Kirillov, SA, Babb, DG, Volkov, DL, Lukovich, JV, Tao, R, Ehn, JK, Sydor, K, Barber, DG.** 2020. Atmospheric vorticity sets the basin-scale circulation in Hudson Bay. *Elementa: Science of the Anthropocene* **8**(1). DOI: <http://dx.doi.org/10.1525/elementa.049>.
- Donnelly, C, Andersson, JCM, Arheimer, B.** 2016. Using flow signatures and catchment similarities to evaluate the E-HYPE multi-basin model across Europe. *Hydrological Sciences Journal* **61**(2): 255–273. DOI: <http://dx.doi.org/10.1080/02626667.2015.1027710>.
- Dukhovskoy, DS, Myers, PG, Platov, G, Timmermans, ML, Curry, B, Proshutinsky, A, Bamber, JL, Chassignet, E, Hu, X, Lee, CM, Somavilla, R.** 2016. Greenland freshwater pathways in the sub-Arctic Seas from model experiments with passive tracers. *Journal of Geophysical Research: Oceans* **121**(1): 877–907. DOI: <http://dx.doi.org/10.1002/2015JC011290>.
- Durocher, M, Burn, DH, Mosto, S.** 2018. A nationwide regional flood frequency analysis at ungauged sites using ROI / GLS with copulas and super regions. *Journal of Hydrology* **567**: 191–202. DOI: <http://dx.doi.org/10.1016/j.jhydrol.2018.10.011>.
- Durocher, M, Requena, A, Burn, DH, Pellerin, J.** 2019. Analysis of trends in annual streamflow to the Arctic Ocean. *Hydrological Processes* **33**(7): 1143–1151. DOI: <http://dx.doi.org/10.1002/hyp.13392>.
- Dynesius, M, Nilsson, C.** 1994. Fragmentation and flow regulation of river systems in the northern third of the world. *Science* **266**(5186): 753–762. DOI: <http://dx.doi.org/10.1126/science.266.5186.753>.
- Gelfan, A, Gustafsson, D, Motovilov, Y, Arheimer, B, Kalugin, A, Krylenko, I, Lavrenov, A.** 2017. Climate change impact on the water regime of two great Arctic rivers: Modeling and uncertainty issues. *Climatic Change* **141**(3): 499–515. Springer Netherlands. DOI: <http://dx.doi.org/10.1007/s10584-016-1710-5>.
- Grill, G, Lehner, B, Lumsdon, AE, Macdonald, GK, Zarfl, C, Reidy Liermann, C.** 2015. An index-based framework for assessing patterns and trends in river fragmentation and flow regulation by global dams at multiple scales. *Environmental Research Letters* **10**(1): 015001. DOI: <http://dx.doi.org/10.1088/1748-9326/10/1/015001>.
- Groisman, PY, Sherstyukov, BG, Razuvaev, VN, Knight, RW, Enloe, JG, Stroumentova, NS, Whitfield, PH, Førland, E, Hannsen-Bauer, I, Tuomenvirta, H, Aleksandersson, H.** 2007. Potential forest fire danger over Northern Eurasia: Changes during the 20th century. *Global and Planetary Change* **56**(3–4): 371–386. DOI: <http://dx.doi.org/10.1016/j.gloplacha.2006.07.029>.
- Gupta, HV, Kling, H, Yilmaz, KK, Martinez, GF.** 2009. Decomposition of the mean squared error and NSE performance criteria: Implications for improving

- hydrological modelling. *Journal of Hydrology* **377**(1–2): 80–91.
- Haine, TW, Curry, B, Gerdes, R, Hansen, E, Karcher, M, Lee, C, Rudels, B, Spreen, G, de Steur, L, Stewart, KD, Woodgate, R.** 2015. Arctic freshwater export: Status, mechanisms, and prospects. *Global and Planetary Change* **125**: 13–35. DOI: <http://dx.doi.org/10.1016/j.gloplacha.2014.11.013>.
- Hamilton, A, Moore, R.** 2013. Winter streamflow variability in two groundwater-fed sub-Arctic rivers, Yukon Territory, Canada. *Canadian Journal of Civil Engineering* **37**(1): 3–21. DOI: <http://dx.doi.org/10.4296/cwrj3701865>.
- Holland, MM, Bitz, CM.** 2003. Polar amplification of climate change in coupled models. *Climate Dynamics* **21**(3–4): 221–232. DOI: <http://dx.doi.org/10.1007/s00382-003-0332-6>.
- Huss, M, Farinotti, D.** 2012. Distributed ice thickness and volume of all glaciers around the globe. *Journal of Geophysical Research: Earth Surface* **117**(4). DOI: <http://dx.doi.org/10.1029/2012JF002523>.
- Ilicak, M, Drange, H, Wang, Q, Gerdes, R, Aksenov, Y, Bailey, D, Bentsen, M, Biastoch, A, Bozec, A, Böning, C, Cassou, C.** 2016. An assessment of the Arctic Ocean in a suite of interannual CORE-II simulations. Part III: Hydrography and fluxes. *Ocean Modelling* **100**: 141–161. DOI: <http://dx.doi.org/10.1016/j.ocemod.2016.02.004>.
- Jafarov, EE, Coon, ET, Harp, DR, Wilson, CJ, Painter, SL, Atchley, AL.** 2018. Modeling the role of preferential snow accumulation in through talik development and hillslope groundwater flow in a transitional permafrost landscape. *Environmental Research Letters* **13**(10). DOI: <http://dx.doi.org/10.1088/1748-9326/aadd30>.
- Kendall, MG.** 1975. Rank correlation measures. *Charles Griffin, London* **202**: 15.
- Klemeš, V.** 1997. Of carts and horses in hydrologic modeling. *Journal of Hydrologic Engineering* **2**: 43–49. DOI: [http://dx.doi.org/10.1061/\(ASCE\)1084-0699\(1997\)2:2\(43\)](http://dx.doi.org/10.1061/(ASCE)1084-0699(1997)2:2(43)).
- Koirala, S, Hirabayashi, Y, Mahendran, R, Kanae, S.** 2014. Global assessment of agreement among streamflow projections using CMIP5 model outputs. *Environmental Research Letters* **9**(6). DOI: <http://dx.doi.org/10.1088/1748-9326/9/6/064017>.
- Kottek, M, Grieser, J, Beck, C, Rudolf, B, Rubel, F.** 2006 Jul 10. World Map of the Köppen-Geiger climate classification updated. *Meteorol Zeitschrift*: 259–263. DOI: <http://dx.doi.org/10.1127/0941-2948/2006/0130>.
- Lambert, E, Nummelin, A, Pemberton, P, Ilicak, M.** 2019. Tracing the Imprint of river runoff variability on Arctic water mass transformation. *Journal of Geophysical Research: Oceans* **124**(1): 302–319. DOI: <http://dx.doi.org/10.1029/2017JC013704>.
- Lindström, G, Pers, C, Rosberg, J, Strömqvist, J, Arheimer, B.** 2010. Development and testing of the HYPE (hydrological predictions for the environment) water quality model for different spatial scales. *Hydrology Research* **41**(3–4): 295–319.
- Lukovich, JV, Jafarikhasragh, S, Myers, PG, Marson, J, Pennelly, C, Stroeve, JC, Sydor, K, Wong, K, Stadnyk, TA, Barber, DG.** n.d. Simulated relative climate change and regulation impacts on sea ice and oceanographic conditions in the Hudson Bay Complex. *Elementa: Sciences of the Anthropocene* (submitted: ELEMENTA-D-20-00127)
- MacDonald, MK, Stadnyk, TA, Déry, SJ, Braun, M, Gustafsson, D, Isberg, K, Arheimer, B.** 2018. Impacts of 1.5 and 2.0°C warming on pan-Arctic river discharge into the Hudson Bay Complex through 2070. *Geophysical Research Letters* **45**(15). DOI: <http://dx.doi.org/10.1029/2018GL079147>.
- Makarieva, O, Shikhov, A, Nesterova, N, Ostashov, A.** 2019. Historical and recent aufeis in the Indigirka River basin (Russia). *Earth System Science Data* **11**: 409–420. DOI: <http://dx.doi.org/10.5194/essd-11-409-2019>.
- Mann, HB.** 1945. Nonparametric tests against trend. *Econometrica* **13**(3): 245. JSTOR. DOI: <http://dx.doi.org/10.2307/1907187>.
- McClelland, JW, Holmes, RM, Peterson, BJ, Stieglitz, M.** 2004. Increasing river discharge in the Eurasian Arctic: Consideration of dams, permafrost thaw, and fires as potential agents of change. *Journal of Geophysical Research: Atmospheres* **109**(18). DOI: <http://dx.doi.org/10.1029/2004JD004583>.
- Moriasi, DN, Gitau, MW, Pai, N, Daggupati, P.** 2016. Hydrologic and water quality models: Performance measures and evaluation criteria. *Transactions of the ASABE* **58**(6): 1763–1785. DOI: <http://dx.doi.org/10.13031/trans.58.10715>.
- Morison, J, Kwok, R, Peralta-Ferriz, C, Alkire, M, Rigor, I, Andersen, R, Steele, M.** 2012. Changing Arctic Ocean freshwater pathways. *Nature* **481**(7379): 66–70. DOI: <http://dx.doi.org/10.1038/nature10705>.
- Nummelin, A, Ilicak, M, Li, C, Smedsrud, LH.** 2016. Consequences of future increased Arctic runoff on Arctic Ocean stratification, circulation, and sea ice cover. *Journal of Geophysical Research: Oceans* **121**(1): 617–637. DOI: <http://dx.doi.org/10.1002/2015JC011156>.
- Nummelin, A, Li, C, Smedsrud, LH.** 2015. Response of Arctic Ocean stratification to changing river runoff in a column model. *Journal of Geophysical Research: Oceans* **120**(4): 2655–2675. DOI: <http://dx.doi.org/10.1002/2014JC010571>.
- Pemberton, P, Nilsson, J.** 2016. The response of the central Arctic Ocean stratification to freshwater perturbations. *Journal of Geophysical Research: Oceans* **121**(1): 792–817. DOI: <http://dx.doi.org/10.1002/2015JC011003>.
- Peterson, BJ, Holmes, RM, McClelland, JW, Vörösmarty, CJ, Lammers, RB, Shiklomanov, AI, Shiklomanov, IA, Rahmstorf, S.** 2002. Increasing river discharge to the Arctic Ocean. *Science* **298**(5601): 2171–2173. DOI: <http://dx.doi.org/10.1126/science.1077445>.

- Pizzolato, L, Howell, SEL, Derksen, C, Dawson, J, Copland, L.** 2014. Changing sea ice conditions and marine transportation activity in Canadian Arctic waters between 1990 and 2012. *Climatic Change* **123**(2): 161–173. DOI: <http://dx.doi.org/10.1007/s10584-013-1038-3>.
- Pohl, E, Grenier, C, Vrac, M, Kageyama, M.** 2020. Emerging climate signals in the Lena River catchment: a non-parametric statistical approach. *Hydrology and Earth System Sciences* **24**(5): 2817–2839. DOI: <http://dx.doi.org/10.5194/hess-24-2817-2020>.
- Pohl, S, Marsh, P, Bonsal, BR.** 2007. Modelling the impact of climate change on runoff and annual water balance of an Arctic headwater basin. *Arctic* **60**(2): 173–186.
- Pokorny, S, Stadnyk, TA, Ali, G, Lihare, R, Déry, SJ, Koenig, K.** 2021. Cumulative effects of uncertainty on simulated streamflow in a hydrologic modeling environment. *Elementa: Science of the Anthropocene* **9**(1). DOI: <http://dx.doi.org/10.1525/elementa.431>.
- Pozdnyakov, DV, Johannessen, OM, Korosov, AA, Pettersson, LH, Grassl, H, Miles, MW.** 2007. Satellite evidence of ecosystem changes in the White Sea: A semi-enclosed Arctic marginal shelf sea. *Geophysical Research Letters* **34**(8). DOI: <http://dx.doi.org/10.1029/2006GL028947>.
- Proshutinsky, A, Krishfield, R, Toole, JM, Timmermans, ML, Williams, W, Zimmermann, S, Yamamoto-Kawai, M, Armitage, TWK, Dukhovskoy, D, Golubeva, E, Manucharyan, GE, Platov, G, Watanabe, E, Kikuchi, T, Nishino, S, Itoh, M, Kang, S-H, Cho, K-H, Tateyama, K, Zhao, J.** 2019. Analysis of the Beaufort Gyre freshwater content in 2003–2018. *Journal of Geophysical Research: Oceans* **124**(12): 9658–9689. DOI: <http://dx.doi.org/10.1029/2019JC015281>.
- Prowse, TD, Wrona, FJ, Reist, JD, Gibson, JJ, Hobbie, JE, Le, LMJ, Vincent, WF.** 2006. Climate change effects on hydroecology of Arctic freshwater ecosystems. *AMBIO: A Journal of the Human Environment* **35**(7): 347–358.
- Rabe, B, Karcher, M, Schauer, U, Toole, JM, Krishfield, RA, Pisarev, S, Kauker, F, Gerdes, R, Kikuchi, T.** 2011. An assessment of Arctic Ocean freshwater content changes from the 1990s to the 2006–2008 period. *Deep Sea Research Part I: Oceanographic Research Papers* **58**(2): 173–185. DOI: <http://dx.doi.org/10.1016/j.dsr.2010.12.002>.
- Rennermalm, AK, Wood, EF, Troy, TJ.** 2010. Observed changes in pan-Arctic cold-season minimum monthly river discharge. *Climate Dynamics* **35**: 923–939. DOI: <http://dx.doi.org/10.1007/s00382-009-0730-5>.
- Ridenour, NA, Hu, X, Jafarikhasragh, S, Landy, JC, Lukovich, JV, Stadnyk, TA, Sydor, K, Myers, PG, Barber, DG.** 2019. Sensitivity of freshwater dynamics to ocean model resolution and river discharge forcing in the Hudson Bay Complex. *Journal of Marine Systems* **196**: 48–64. DOI: <http://dx.doi.org/10.1016/j.jmarsys.2019.04.002>.
- Rubel, F, Kottek, M.** 2010. Observed and projected climate shifts 1901–2100 depicted by world maps of the Koppen-Geiger climate classification. *Meteorol Zeitschrift* **19**(2): 135–141.
- Scheepers, H, Wang, J, Gan, TY, Kuo, CC.** 2018. The impact of climate change on inland waterway transport: Effects of low water levels on the Mackenzie River. *Journal of Hydrology* **566**: 285–298. DOI: <http://dx.doi.org/10.1016/j.jhydrol.2018.08.059>.
- Semiletov, IP, Pipko, II, Shakhova, NE, Dudarev, OV, Pugach, SP, Charkin, AN, McRoy, CP, Kosmach, D, Gustafsson, Ö.** 2011. Carbon transport by the Lena River from its headwaters to the Arctic Ocean, with emphasis on fluvial input of terrestrial particulate organic carbon vs. carbon transport by coastal erosion. *Biogeosciences* **8**(9): 2407–2426. DOI: <http://dx.doi.org/10.5194/bg-8-2407-2011>.
- Serreze, MC, Barry, RG.** 2014. *The Arctic climate system*. 2nd ed. Cambridge, UK: Cambridge University Press. DOI: <http://dx.doi.org/10.1017/CBO9781139583817>.
- Shiklomanov, AI, Lammers, RB.** 2009. Record Russian river discharge in 2007 and the limits of analysis. *Environmental Research Letters* **4**(4): 045015. DOI: <http://dx.doi.org/10.1088/1748-9326/4/4/045015>.
- Sibert, V, Zakardjian, B, Saucier, F, Gosselin, M, Starr, M, Senneville, S.** 2010. Spatial and temporal variability of ice algal production in a 3D ice–ocean model of the Hudson Bay, Hudson Strait and Foxe Basin system. *Polar Research* **29**(3): 353–378. DOI: <http://dx.doi.org/10.3402/polar.v29i3.6084>.
- Smith, LC, Sheng, Y, MacDonald, GM, Hinzman, LD.** 2005. Disappearing Arctic lakes. *Science* **308**(5727): 1429. DOI: <http://dx.doi.org/10.1126/science.1108142>.
- Stadnyk, TA, Dery, SJ, MacDonald, M, Koenig, K.** 2019. The Freshwater System, in Kuzyk ZZ, Candlish LM, eds., *Integrated regional impact study: Hudson Bay*. 113–154. Available at <https://arcticnet.ulaval.ca/docs/IRIS3-HudsonBay-VF.pdf>. Accessed 1 May 2021.
- Stadnyk, TA, MacDonald, MK, Tefs, A, Déry, SJ, Koenig, K, Gustafsson, D, Isberg, K, Arheimer, B.** 2020. Hydrological modeling of freshwater discharge into Hudson Bay using HYPE. *Elementa: Science of the Anthropocene* **8**. DOI: <http://dx.doi.org/10.1525/elementa.439>.
- Straneo, F, Heimbach, P.** 2013. North Atlantic warming and the retreat of Greenland’s outlet glaciers. *Nature* **504**(7478): 36–43. DOI: <http://dx.doi.org/10.1038/nature12854>.
- Stroeve, J, Notz, D.** 2018. Changing state of Arctic sea ice across all seasons. *Environmental Research Letters* **13**(10): 103001. DOI: <http://dx.doi.org/10.1088/1748-9326/aade56>.
- Swedish Meteorological and Hydrologic Institute.** 2020. Arctic-HYPE version 3.0.26. Hypeweb.

- Available at https://hypeweb.smhi.se/wp-content/uploads/2019/04/model_arctichype_3_0_26.pdf. Accessed 16 June 2020.
- Tang, W, Yueh, SH, Yang, D, Mcleod, E, Fore, A, Hayaishi, A, Olmedo, E, Martínez, J, Gabarró, C.** 2020. The potential of space-based sea surface salinity on monitoring the Hudson Bay freshwater cycle. *Remote Sensing* **12**(5). DOI: <http://dx.doi.org/10.3390/rs12050873>.
- Tefs, AAG.** 2018. *Simulating hydroelectric regulation and climate change in the Hudson Bay drainage basin*. Department of Civil Engineering, University of Manitoba, Winnipeg, Manitoba, Canada.
- Tefs, AAG, Stadnyk, TA, Koenig, KA, Dery, SJ, Macdonald, MK, Hamilton, M, Slota, P, Crawford, J.** 2021. Simulating river regulation and reservoir performance in a continental-scale hydrologic model. *Environmental Modelling & Software* (in press). DOI: http://dx.doi.org/ENVSOF2019_485_R2.
- Thornalley, DJ, Oppo, DW, Ortega, P, Robson, JI, Briereley, CM, Davis, R, Hall, IR, Moffa-Sanchez, P, Rose, NL, Spooner, PT, Yashayaev, I.** 2018. Anomalous weak Labrador Sea convection and Atlantic overturning during the past 150 years. *Nature* **556**(7700): 227–230. DOI: <http://dx.doi.org/10.1038/s41586-018-0007-4>.
- Van Vliet, MTH, Ludwig, F, Zwolsman, JGG, Weedon, GP, Kabat, P.** 2011. Global river temperatures and sensitivity to atmospheric warming and changes in river flow. *Water Resources Research* **47**(2). DOI: <http://dx.doi.org/10.1029/2010WR009198>.
- Velicogna, I, Sutterley, TC, van den Broeke, MR.** 2014. Regional acceleration in ice mass loss from Greenland and Antarctica using GRACE time-variable gravity data. *Geophysical Research Letters* **41**(22): 8130–8137. DOI: <http://dx.doi.org/10.1002/2014GL061052>.
- Vörösmarty, CJ, Meybeck, M, Fekete, B, Sharma, K, Green, P, Syvitski, JP.** 2003. Anthropogenic sediment retention: Major global impact from registered river impoundments. *Global and Planetary Change* **39**(1–2): 169–190.
- Wang, G, Zhao, C, Xu, J, Qiao, F, Xia, C.** 2016. Verification of an operational ocean circulation-surface wave coupled forecasting system for the China's seas. *Acta Oceanologica Sinica* **35**(2): 19–28. DOI: <http://dx.doi.org/10.1007/s13131-016-0810-4>.
- Wang, H, Legg, S, Hallberg, R.** 2018. The effect of Arctic freshwater pathways on North Atlantic convection and the Atlantic meridional overturning circulation. *Journal of Climate* **31**(13): 5165–5188. DOI: <http://dx.doi.org/10.1175/JCLI-D-17-0629.1>.
- Westerberg, IK, Sikorska-Senoner, AE, Viviroli, D, Vis, M, Seibert, J.** 2020 Apr 30. Hydrological model calibration with uncertain discharge data. *Hydrological Sciences Journal*: 1–16. DOI: <http://dx.doi.org/10.1080/02626667.2020.1735638>.
- Woodgate, RA, Aagaard, K, Weingartner, TJ.** 2006. Interannual changes in the Bering Strait fluxes of volume, heat and freshwater between 1991 and 2004. *Geophysical Research Letters* **33**(15). DOI: <http://dx.doi.org/10.1029/2006GL026931>.
- Yang, Q, Dixon, TH, Myers, PG, Bonin, J, Chambers, D, Van Den Broeke, MR.** 2016. Recent increases in Arctic freshwater flux affects Labrador Sea convection and Atlantic overturning circulation. *Nature Communications* **7**(1): 1–8. DOI: <http://dx.doi.org/10.1038/ncomms10525>.
- Yue, S, Pilon, P, Phinney, B, Cavadias, G.** 2002. The influence of autocorrelation on the ability to detect trend in hydrological series. *Hydrological Processes* **16**(9): 1807–1829. DOI: <http://dx.doi.org/10.1002/hyp.1095>.
- Zhang, X, He, J, Zhang, J, Polyakov, I, Gerdes, R, Inoue, J, Wu, P.** 2013. Enhanced poleward moisture transport and amplified northern high-latitude wetting trend. *Nature Climate Change* **3**(1): 47–51. DOI: <http://dx.doi.org/10.1038/nclimate1631>.

How to cite this article: Stadnyk, TA, Tefs, A, Broesky, M, Déry, SJ, Myers, PG, Ridenour, NA, Koenig, K, Vonderbank, L, Gustafsson, D. 2021. Changing freshwater contributions to the Arctic: A 90-year trend analysis (1981–2070). *Elementa: Science of the Anthropocene* 9(1). DOI: <https://doi.org/10.1525/elementa.2020.00098>

Domain Editor-in-Chief: Jody W. Deming, University of Washington, Seattle, WA, USA

Associate Editor: Mary-Louise Timmermans, Yale University, New Haven, CT, USA

Knowledge Domain: Ocean Science

Part of an Elementa Special Feature: BaySys

Published: May 28, 2021 **Accepted:** April 13, 2021 **Submitted:** July 03, 2020

Copyright: © 2021 The Author(s). This is an open-access article distributed under the terms of the Creative Commons Attribution 4.0 International License (CC-BY 4.0), which permits unrestricted use, distribution, and reproduction in any medium, provided the original author and source are credited. See <http://creativecommons.org/licenses/by/4.0/>.



Elem Sci Anth is a peer-reviewed open access journal published by University of California Press.

OPEN ACCESS 

Copyright of Elementa: Science of the Anthropocene is the property of Ubiquity Press and its content may not be copied or emailed to multiple sites or posted to a listserv without the copyright holder's express written permission. However, users may print, download, or email articles for individual use.